

# Needle in a Haystack: Finding Supermassive Black Hole-related Flares in the Zwicky Transient Facility Public Survey

Yael Dgany<sup>1</sup> , Iair Arcavi<sup>1,2</sup> , Lydia Makrygianni<sup>1</sup> , Craig Pellegrino<sup>3,4</sup> , and D. Andrew Howell<sup>3,4</sup> 

The School of Physics and Astronomy, Tel Aviv University, Tel Aviv 69978, Israel; [arcavi@tauex.tau.ac.il](mailto:arcavi@tauex.tau.ac.il)

<sup>2</sup> CIFAR Azrieli Global Scholars program, CIFAR, Toronto, Canada

<sup>3</sup> Las Cumbres Observatory, 6740 Cortona Drive, Suite 102, Goleta, CA 93117-5575, USA

<sup>4</sup> Department of Physics, University of California, Santa Barbara, CA 93106-9530, USA

Received 2023 February 15; revised 2023 July 15; accepted 2023 July 17; published 2023 October 27

## Abstract

Transient accretion events onto supermassive black holes (SMBHs), such as tidal disruption events (TDEs), Bowen Fluorescence Flares (BFFs), and active galactic nuclei (AGNs), which are accompanied by sudden increases of activity, offer a new window onto the SMBH population, accretion physics, and stellar dynamics in galaxy centers. However, such transients are rare and finding them in wide-field transient surveys is challenging. Here we present the results of a systematic real-time search for SMBH-related transients in Zwicky Transient Facility (ZTF) public alerts, using various search queries. We examined 345 rising events coincident with a galaxy nucleus, with no history of previous activity, of which 223 were spectroscopically classified. Of those, five (2.2%) were TDEs, one (0.5%) was a BFF, and two (0.9%) were AGN flares. Limiting the search to blue events, the fraction of TDEs nearly doubles to 4.1%, and no TDEs are missed. Limiting the search further to candidate post-starburst galaxies increases the relative number of TDEs to 16.7%, but the absolute numbers in such a search are small. The main contamination source is supernovae (95.1% of classified events), of which the majority (82.2% of supernovae) are of Type Ia. In a comparison set of 39 events with limited photometric history, the AGN contamination increases to  $\sim 30\%$ . Host galaxy offset is not a significant discriminant of TDEs in current ZTF data, but might be useful in higher-resolution data. Our results can be used to quantify the efficiency of various SMBH-related transient search strategies in optical surveys such as ZTF and the Legacy Survey of Space and Time.

*Unified Astronomy Thesaurus concepts:* Supernovae (1668); Tidal disruption (1696); Supermassive black holes (1663); Active galactic nuclei (16); Astronomical methods (1043)

*Supporting material:* machine-readable table

## 1. Introduction

Wide-field optical surveys have recently found new types of transients occurring exclusively in galaxy centers. These transients are thought to be associated with enhanced accretion events onto supermassive black holes (SMBHs). As such, they have the potential to reveal the presence and properties of otherwise inactive SMBHs, as well as constrain physics of accretion and related radiative processes. Notable examples of such transients are optical-ultraviolet tidal disruption events (TDEs) and Bowen Fluorescence Flares (BFFs). Both types of events are characterized by a sudden increase of flux by several orders of magnitude and are thus much more dramatic than the few tens of percent level of variability seen in most active galactic nuclei (AGNs), which host SMBHs with steadily accreting material.

A TDE is the result of the disruption of a star by an SMBH (Hills 1975). In such an event, half of the stellar material is expected to accrete onto the SMBH (Rees 1988). For disruptions occurring outside the event horizon (expected for solar-type stars disrupted by SMBHs of masses  $\lesssim 10^8 M_\odot$ , for example), the accretion event will be accompanied by an observable flare. Several such flares have been detected in

X-rays, as expected from directly observed accretion emission (see Saxton et al. 2020 for a recent review). However, somewhat surprisingly, a class of optical-ultraviolet TDEs has also been discovered (Gezari et al. 2012; Arcavi et al. 2014). These events are mostly blue, with blackbody temperatures of a few  $10^4$  K lasting for several months to years, and show broad emission lines of H and/or He in their spectra. The emission mechanism leading to these observed properties is a topic of active debate (see van Velzen et al. 2020 and Gezari 2021 for recent reviews).

In addition to their emission mechanism puzzle, optical-ultraviolet TDEs show a peculiar and strong host galaxy preference for post-starburst galaxies (Arcavi et al. 2014; French et al. 2016, 2020b). This preference is not yet fully understood, but might be related to the spatial distribution and dynamics of various stellar populations in the centers of such galaxies (French et al. 2020a). Studying optical-ultraviolet TDEs can thus also help shed light on the stellar dynamics in galaxy nuclei, which are responsible for driving up TDE rates in post-starburst environments (e.g., Madigan et al. 2018).

Like TDEs, BFFs are also blue and show H and He lines in their spectra, leading Tadhunter et al. (2017) to classify the first such observed event as a TDE. However, a second (Gromadzki et al. 2019) and then third (Trakhtenbrot et al. 2019) event showed that their typical spectral line widths are much narrower than those of TDEs, and that their light curves decline much more slowly than those of TDEs. This led



Original content from this work may be used under the terms of the [Creative Commons Attribution 4.0 licence](https://creativecommons.org/licenses/by/4.0/). Any further distribution of this work must maintain attribution to the author(s) and the title of the work, journal citation and DOI.

Trakhtenbrot et al. (2019) to classify BFFs as a separate observational class. There are now also hints that BFFs occur in previously existing AGNs (Makrygianni et al. 2023), meaning that they could be the result of accretion instabilities in an AGN disk or of a TDE occurring in an AGN and interacting with its existing accretion disk (e.g., Chan et al. 2019).

BFFs are named as such because they exhibit certain emission lines (such as He II 4686 Å and N III 4640 Å, among others) that are associated with the Bowen fluorescence mechanism (Bowen 1928). In this mechanism, extreme-ultraviolet and X-ray photons excite certain He II transitions, which in turn launch a cascade of transitions observed in the optical and ultraviolet regimes. This process requires the presence of extreme-ultraviolet photons hitting high-density and high-optical-depth material, and it was indeed predicted decades ago to occur in AGNs (Netzer et al. 1985). Since the identification of this mechanism in BFFs, it has also been suggested to occur in some TDEs (Blagorodnova et al. 2019; Leloudas et al. 2019), hinting at a possible connection between the conditions of matter and radiation in these two types of events related to SMBH accretion.

It is clear that studying more TDEs and BFFs is necessary in order to better constrain their nature, emission mechanisms, and the physics they can teach us in relation to SMBHs and their associated accretion processes. However, these events are intrinsically rare. The exact TDE rate remains uncertain, but is likely to be in the range of  $10^{-5}$ – $10^{-4}$  events per galaxy per year (e.g., Wang & Merritt 2004; Stone & Metzger 2016). The BFF rate is not yet estimated at all, but observationally, they are less common than TDEs (this could be due in large part to selection effects, as discussed below). In addition to their intrinsic rarity, finding TDEs and BFFs is also observationally challenging. As events that occur in galaxy centers, their detection is contaminated by image-subtraction artifacts, “regular” AGN activity, unresolved non-SMBH-related transients, and even variable stars that cannot be easily distinguished from distant or compact galaxies. For these reasons, only a few dozen TDEs and a few BFFs have been identified so far.

Attempts have been made to devise selection criteria to weed out such transients from the large alert streams produced by wide-field transient surveys. Such criteria typically include selecting candidates by the significance of the flare (since TDEs and BFFs are luminous), color (since TDEs and BFFs are blue), and host properties (since TDE hosts are mostly quiescent).

Hung et al. (2018) searched a set of 493 nuclear transients (0.8'' from their host galaxy center) from the intermediate Palomar Transient Factory, for events with  $g - R < 0$  mag residing in galaxies with  $u - g > 1$  mag and  $g - r > 0.5$  mag. These cuts reduced the set of candidates to just 26, of which two are TDEs. Still, the contamination fraction is large. A substantial amount of telescope time is required to vet 13 candidates (through spectroscopy or ultraviolet colors) for each bona fide TDE.

One way to further reduce the amount of transient contamination in TDE searches is to focus the search on galaxies most similar to the post-starburst hosts that TDEs seem to prefer. French & Zabludoff (2018) used galaxies from the Sloan Digital Sky Survey (SDSS; York et al. 2000) Data Release 12 main galaxy survey (Strauss et al. 2002; Alam et al. 2015), with similar spectral properties as those of actual TDE

hosts, to train a machine-learning algorithm to identify such galaxies from photometry alone. They then used this algorithm to identify several tens of thousands of TDE host galaxy candidates in archival survey data. Arcavi et al. (2022c) found indeed that using the French & Zabludoff (2018) catalog of galaxies reduces contamination by roughly a factor of 3–50 (depending on the subset of galaxies used from the catalog) compared to filtering just on quiescent galaxies, and that the only contaminant transients in such galaxies are Type Ia supernovae (SNe). That study, however, was based on archival data alone.

Here we perform a systematic real-time search for TDEs, BFFs, and other possible SMBH flares in the Zwicky Transient Facility (ZTF; Bellm 2014; Graham et al. 2019) alert stream, as parsed by the Lasair broker (Smith et al. 2019). We use various search criteria that rely on candidate brightness and color and their host galaxy properties, and compare their effectiveness in selecting TDEs and BFFs against actual spectroscopic classifications obtained by us and by the rest of the community. We focus on rising events (i.e., events discovered before their peak), selected using visual inspection, for two main reasons. First, such events are more scientifically valuable, as they include the peak time and brightness, as well as the early pre-peak emission, both of which contain important information for constraining models of SNe and TDEs. In addition, rising events present a way of decreasing the number of events to a more manageable subsample for spectroscopic classification, while avoiding biasing the sample toward a particular class (the selection of rising events is done before their classifications are known).<sup>5</sup>

Our goal is to quantify the contamination fraction for the various search criteria and to check whether any of them miss TDEs and BFFs. Here, we do not constrain the intrinsic rates of SNe, TDEs, or BFFs in nature, but rather the observed fractions of events, to help guide searches in ongoing and future transient surveys and to help prioritize limited spectroscopic classification resources. We detail our search criteria in Section 2, present and analyze our results in Section 3, and discuss them and conclude in Section 4.

## 2. Methods

We searched the ZTF real-time alert stream for transients in galaxy centers every day between 2020 November 3 and 2022 March 6 (UT dates), with the exception of a ~2 month break due to a ZTF technical outage between 2021 December 5 and 2022 February 17. In total, our search includes alerts from 414 days. We used the custom query builder on version 1.0 of the Lasair broker<sup>6</sup> to filter the alerts. Lasair uses a contextual classifier called *Sherlock*.<sup>7</sup> *Sherlock* is a boosted decision tree algorithm that provides an initial classification of every nonmoving object by performing a spatial crossmatch against data from historical and ongoing astronomical surveys, including catalogs of nearby galaxies, variable stars, and AGNs (see Section 4.2 of Smith et al. 2020 for more details).

<sup>5</sup> One exception is that we would be less likely to catch rapidly rising events during their rise compared to slower-rising events, but the typical ZTF public survey cadence is  $\lesssim 3$  days, which should be enough to catch most rapidly evolving transients (e.g., Ho et al. 2023).

<sup>6</sup> <https://lasair.lsst.ac.uk>

<sup>7</sup> [https://lasair.readthedocs.io/en/develop/core\\_functions/sherlock.html](https://lasair.readthedocs.io/en/develop/core_functions/sherlock.html)

Our queries, which are based on the TDE queries by M. Nicholl on version 1.0 of Lasair,<sup>8</sup> filter ZTF alerts according to the following criteria (for each, we state the corresponding Lasair query condition):

1. The candidate is within a certain threshold distance of the nearest Sherlock catalog source. For 80% of our sample, we choose a threshold of  $0''.5$ .<sup>9</sup> For the rest, we increased the separation threshold to  $1''$  to check if this has a strong effect on the results:

```
sherlock_classifications.separationArcsec < 0.5
or
sherlock_classifications.separationArcsec < 1.
```

We found that the value of the threshold has no significant effect on the results (see the Appendix B) and therefore analyzed the joint sample of both separation thresholds together to increase our sample size. This condition, regardless of the separation threshold, filters out “hostless” events, i.e., those with no host in the Sherlock catalog.

2. The nearest catalog source is likely a galaxy rather than a star:<sup>10</sup>

```
objects.sgscore1 < 0.5.
```

3. The Sherlock classification of the candidate is either “SN” (Supernova) or “NT” (Nuclear Transient):<sup>11</sup>

```
sherlock_classifications.classification in (''SN'', ''NT'').
```

4. The candidate does not have detections more than 100 days ago (indicating that it might be a variable, rather than a transient source, though some past detections could be artifacts):<sup>12</sup>

```
objects.jdmin > JDNOW() - 100.
```

5. The candidate does not have a ZTF17 or ZTF19 name, meaning that it was not created by ZTF in 2017 or 2019 (this is another way of filtering out variable sources):<sup>13</sup>

```
objects.objectId NOT LIKE 'ZTF17%' AND objects.objectId NOT LIKE 'ZTF19%'.  
8 https://lasair.roe.ac.uk/filters/94/ and https://lasair.roe.ac.uk/filters/95/.
```

<sup>9</sup> This value was chosen given that the ZTF pixel scale of  $1''$  per pixel results in a typical centroiding accuracy of  $\lesssim 0''.3$ , which we increase to  $0''.5$  to be inclusive.

<sup>10</sup> `sgscore1` is based on a random forest classifier trained and implemented in the ZTF alerts by Tachibana & Miller (2018). An `sgscore` value closer to 0 means that the nearest source in the Panoramic Survey Telescope and Rapid Response System (Kaiser et al. 2010) first survey (PS1; Chambers et al. 2016) catalog is more likely a galaxy, while a value closer to 1 means it is more likely a star.

<sup>11</sup> The other Sherlock classifications, which we exclude from our search, are: “VS” (Variable Star), “CV” (Cataclysmic Variable), “BS” (Bright Star), “AGN,” “Orphan,” (if the transient fails to match against any cataloged source), and “Unclear.”

<sup>12</sup> A ZTF alert is reported to the brokers with a 30 day history, which may contain prediscovery detections. Lasair marks the time of the first detection in this 30 day history as `jdmin`.

<sup>13</sup> Sporadic false detections in galaxy centers may occur, sometimes years before a real event occurs at the same position, and based on false detections that are later filtered out by the brokers. In such a case, the real event would have an old name from when the false detection occurred years before. Removing such events might thus undesirably filter out interesting candidates. In order to avoid losing many candidates, but still not being inundated with variable sources, we decided to allow events with ZTF18 names (several bad subtractions in 2018 caused false events then; E. Bellm, private communication), while removing those with ZTF17 and ZTF19 names.

6. The candidate is not a previously classified SN: `crossmatch_tns.tns_prefix != 'SN'`.
7. The candidate has  $< 3$  detections deemed unreliable (i.e., which are not marked as good quality and/or the candidate is dimmer than the reference):<sup>14</sup> `objects.ncand---objects.ncandgp < 3`.
8. At least one of those detections was no more than 14 days ago (in order to avoid old objects that might already be fading): `objects.ncandgp_14 > 1`.
9. The candidate is more than  $10^\circ$  away from the Galactic plane (in order to filter stellar flares or variability): `objects.glatmean > 10 OR objects.glatmean < -10`.

Conditions 4 and 5 could introduce a bias against finding BFFs (which might be associated with preexisting AGNs; Makrygianni et al. 2023) and TDEs occurring in AGNs. However, these conditions are necessary in order to remove “normal” AGN activity, which can otherwise be a major contaminant (see below).

In addition to conditions 1–9, we create two variations of the query, each with a different magnitude limit:

- 10a. The latest *g*- or *r*-band magnitude of the candidate is brighter than 19:

```
objects.rmag < 19 OR objects.gmag < 19.
```

- 10b. The latest *g*- or *r*-band magnitude of the candidate is brighter than 19.5:

```
objects.rmag < 19.5 OR objects.gmag < 19.5.
```

The motivation for these variations is due to several spectrographs on dynamically scheduled telescopes (which are ideal for the rapid classification of transients)—such as the Floyds spectrographs (Brown et al. 2013) on the Las Cumbres Observatory Faulkes Telescopes North (FTN) and South (FTS) and the SPectrograph for the Rapid Acquisition of Transients (Piascik et al. 2014) on the Liverpool Telescope—being on 2 m class telescopes, with a typical limiting magnitude of 19. Similarly, the advanced extended Public European Southern Observatory (ESO) Spectroscopic Survey for Transient Objects (ePESSTO+, a continuation of PESSTO; Smartt et al. 2013), responsible for a large number of transient classifications, uses the ESO Faint Object Spectrograph and Camera v2 (Buzzoni et al. 1984) on the 3.6 m New Technology Telescope (NTT) to reach a magnitude of 19.5.

For each of these variations, we create three subvariations: one without any additional conditions, one with an additional condition on the color of the event:

11. The candidate has a  $g - r$  magnitude difference  $< 0.05$  (in order to select only blue events, since TDEs are observed to maintain roughly constant blue colors for months; see

<sup>14</sup> `ncand` is the total number of detections from ZTF, which can be either positive or negative subtraction residuals (i.e., a brightening or fading with respect to the reference image). `ncandgp` counts only “good and positive” detections, i.e., a positive flux with respect to the reference and having a ZTF machine-learning real-bogus score  $> 0.75$ . This criterion requires that most detections are good and positive, but allows for one or two light-curve points with poor real-bogus scores if, for example, the transient was detected when it was very young and the subtraction residuals at the earliest epochs have a low real-bogus score due to a relatively low signal-to-noise ratio.

e.g., van Velzen et al. 2020);<sup>15</sup>  
`objects.g_minus_r < 0.05,`

and, finally, one subvariation that searches for candidates coincident with galaxies from the French & Zabludoff (2018) catalog of likely TDE hosts (hereafter referred to as post-starburst, or PS, galaxies; Arcavi et al. 2014; French et al. 2016), as implemented in the “E + A Galaxies” watchlist<sup>16</sup> on Lasair.

In total we have six queries, which we hereby number as follows:

- I. Conditions 1–9, with a limiting magnitude  $<19$  (Condition 10a), blue (Condition 11), and in a PS galaxy.
- II. Conditions 1–9, with a limiting magnitude  $<19$  (Condition 10a) and blue (Condition 11).
- III. Conditions 1–9, with a limiting magnitude  $<19$  (Condition 10a).
- IV. Conditions 1–9, with a limiting magnitude  $<19.5$  (Condition 10b), blue (Condition 11), and in a PS galaxy.
- V. Conditions 1–9, with a limiting magnitude  $<19.5$  (Condition 10b) and blue (Condition 11).
- VI. Conditions 1–9, with a limiting magnitude  $<19.5$  (Condition 10b).

Obviously, these are not independent, with some queries being subsets of others, and all being subsets of Query VI. These queries produced roughly 30 new candidates per day in total, which we inspected manually. Only those showing a coherently rising light curve were marked as candidates of interest. Candidates not obviously rising at discovery were monitored for an extra epoch of ZTF photometry and checked again. Candidates for which it was still not clear whether they were rising or not were monitored for another week. This step removed events that had a flat, varying, or incoherent light curve, which could be due to “normal” AGN variability, the stellar variability of Galactic objects, or artifacts of the ZTF image-subtraction pipeline. In addition, this removed true transients that were already after their peak luminosity and that are not part of our sample as defined here. Of all our filtering steps, this is the most subjective, as it requires visual inspection, rather than some strict criterion for what constitutes a “coherently rising” light curve. However, by checking each candidate during multiple epochs, we aim to make this step as inclusive as possible. In addition, since this step is performed before the classification of the candidate is known, it should not bias the search against a particular type of transient (except extremely rapidly rising events, with rise times  $\lesssim 3$  days).

After these cuts, we were left with a total of 345 candidates of interest (from our entire 414 day search, i.e.,  $\sim 0.83$  candidates of interest per day, on average), which we attempted to classify spectroscopically within a few days of discovery.

Version 3.0 of Lasair (also known as “Iris”) was released in 2021 March. To improve performance, not all of the information that was available in version 1.0 (such as the full detection histories of all candidate events) was carried over to version 3.0. To check for any differences in query results, we add four more queries that we ran on Lasair 3.0 (Iris) between 2022 April 6 and 2022 August 2 (for a total of 118 days):

<sup>15</sup> The  $g - r$  color is evaluated on the most recent night with positive detections (relative to the reference) in both bands. We choose a threshold of 0.05, to be slightly more conservative than the threshold of 0 suggested by Hung et al. (2018). We do not take into account magnitude errors here.

<sup>16</sup> <https://lasair.roe.ac.uk/watchlist/321/>

VII. Conditions 1–9, with a limiting magnitude  $<19$  (Condition 10a).

VIII. Conditions 1–9, with a limiting magnitude  $<19.5$  (Condition 10b).

IX. Conditions 1–9, with a limiting magnitude  $<19$  (Condition 10a) and in a PS galaxy.

X. Conditions 1–9, with a limiting magnitude  $<19.5$  (Condition 10b) and in a PS galaxy.

Color information was not available as a query parameter in Iris, therefore we cannot filter by condition 11 here. We perform the same manual cuts as above and are left with 39 events, which is an average of 0.33 candidates per day. Version 4.0 of Lasair was released in 2022 May, but we do not test it here.

We obtain a total of 345 candidates of interest from Lasair 1.0 (310 of which from using a separation threshold of  $0''.5$  in Criterion 1, with the rest from using a separation threshold of  $1''$ ) and 39 candidates of interest from Lasair 3.0 (all of which from using a separation threshold of  $1''$ ).

For all those brighter than 19th magnitude, we requested spectra through the Las Cumbres Observatory Floyds spectrographs mounted on the 2 m FTN and FTS telescopes at Haleakala (United States) and Siding Spring (Australia) observatories, respectively. Weather, technical issues, and oversubscription of the telescopes mean that not all the requested spectra were obtained or that some were obtained first by the community and reported to Transient Name Server (TNS).<sup>17</sup> We were able to obtain spectra of 83 candidates of interest, taken through a  $2''$  slit placed on the candidate along the parallactic angle (Filippenko 1982). One-dimensional spectra were extracted and the flux and wavelength were calibrated using the `floyds_pipeline`<sup>18</sup> (Valenti et al. 2013). Fainter targets, accessible from La Silla Observatory, were sent for consideration to the ePESSTO+ collaboration, for classification with the NTT.

All of our classification spectra, as well as those obtained by the ePESSTO+ collaboration, were publicly reported to the TNS. Many of our candidates of interest were classified by other members of the community and also reported to the TNS. In total, 246 of our 384 candidates of interest (64.1%) were classified on the TNS. We take these classifications as reported to the TNS and analyze their distribution in the next section.

### 3. Results and Analysis

The full list of our candidates of interest can be found in Table 8 in Appendix C. The redshift distribution of all classified transients with a determined redshift on the TNS (244 events) is presented in Figure 1.<sup>19</sup> While our queries can in principle find TDEs out to a redshift of  $z \sim 0.16$  (using our magnitude limit of 19.5 and a TDE typical peak absolute magnitude of  $-20$ ; van Velzen et al. 2020), the median redshift of our classified candidates of interest is  $z = 0.069$  and all but one of the TDEs are at redshifts  $z < 0.04$  (the most distant TDE, AT 2022csn, at a redshift of  $z = 0.148$ , is also more luminous than typical TDEs; Y. Dgany et al. 2023, in preparation). The reason that most classified events are much

<sup>17</sup> <http://www.wis-tns.org>

<sup>18</sup> [https://github.com/LCOGT/floyds\\_pipeline](https://github.com/LCOGT/floyds_pipeline)

<sup>19</sup> One classified transient, AT 2022amc, has no redshift determination, since its spectrum consists of a blue continuum with no clearly identifiable lines.

**Table 1**  
Numbers and Fractions of the Classes of Candidates of Interest from the Different Queries

Query	Total Transients	Not Classified	SN	AGN	TDE	Other	Galaxy	BFF	Varstar
Lasair 1.0									
I: <19 Mag, Blue, and in PS	6	1	4	0	1	0	0	0	0
Percentage of All Transients	...	16.67%	66.67%	0	16.67%	0	0	0	0
Percentage of Classified Transients	...	...	80.00%	0	20.00%	0	0	0	0
II: <19 Mag and Blue	116	19	91	0	5	0	1	0	0
Percentage of All Transients	...	16.38%	78.45%	0	4.31%	0	0.86%	0	0
Percentage of Classified Transients	...	...	93.81%	0	5.15%	0	1.03%	0	0
III: <19 Mag	213	41	163	2	5	1	1	0	0
Percentage of All Transients	...	19.25%	76.53%	0.94%	2.35%	0.47%	0.47%	0	0
Percentage of Classified Transients	...	...	94.77%	1.16%	2.91%	0.58%	0.58%	0	0
IV: <19.5 Mag, Blue, and in PS	9	3	5	0	1	0	0	0	0
Percentage of All Transients	...	33.33%	55.56%	0	11.11%	0	0	0	0
Percentage of Classified Transients	...	...	83.33%	0	16.67%	0	0	0	0
V: <19.5 Mag and Blue	193	71	116	0	5	0	1	0	0
Percentage of All Transients	...	36.79%	60.10%	0	2.59%	0	0.52%	0	0
Percentage of Classified Transients	...	...	95.08%	0	4.10%	0	0.82%	0	0
VI: <19.5 Mag	345	121	213	2	5	1	1	1	1
Percentage of All Transients	...	35.07%	61.74%	0.58%	1.45%	0.29%	0.29%	0.29%	0.29%
Percentage of Classified Transients	...	...	95.09%	0.89%	2.23%	0.45%	0.45%	0.45%	0.45%
Lasair 3.0 (Iris)									
VII: <19 Mag in Iris	33	13	14	6	0	0	0	0	0
Percentage of All Transients	...	39.39%	42.42%	18.18%	0	0	0	0	0
Percentage of Classified Transients	...	...	70.00%	30.00%	0	0	0	0	0
VIII: <19.5 Mag in Iris	39	17	16	6	0	0	0	0	0
Percentage of All Transients	...	43.59%	41.03%	15.38%	0	0	0	0	0
Percentage of Classified Transients	...	...	72.73%	27.27%	0	0	0	0	0
IX: <19 Mag, in Iris, and in PS	1	0	0	1	0	0	0	0	0
Percentage of All Transients	...	0	0	100.00%	0	0	0	0	0
Percentage of Classified Transients	...	...	0	100.00%	0	0	0	0	0
X: <19.5 Mag, in Iris, and in PS	2	1	0	1	0	0	0	0	0
Percentage of All Transients	...	50.00%	0	50.00%	0	0	0	0	0
Percentage of Classified Transients	...	...	0	100.00%	0	0	0	0	0

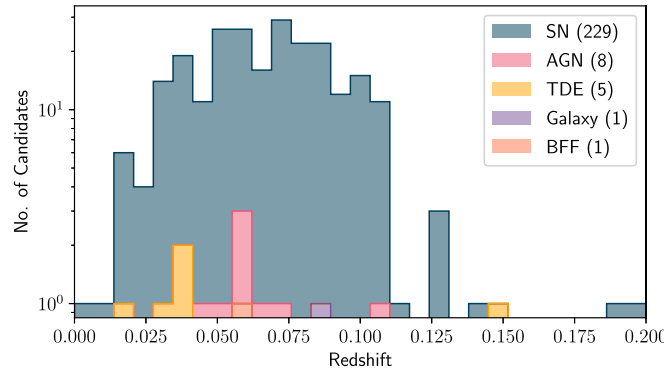


**Figure 1.** Redshift distribution (shown in a stacked histogram) of the 241 classified candidates of interest with redshifts on the TNS. The number of events in each class is denoted in parentheses in the legend.

closer than our redshift limit is likely because nearby events are typically prioritized for spectroscopic classification over more distant events. At the median redshift, our angular cut of 0.5''

from the galaxy nucleus corresponds to a physical cut of  $\sim 0.66$  kpc (assuming the cosmology of Hinshaw et al. 2013).

The distribution of the classifications of our candidates of interest, per query, are listed in Table 1 and presented in Figures 2 and 3. In the interest of simplicity, we consolidate the various SN classifications into one category, which we name “SN.” These include SNe of undetermined type, SNe I of undetermined subtype, SNe Ia and their various subtypes, as well as SNe Ib, Ic, Ic-BL, II, IIn, IIb, and superluminous SNe (SLSNe) of Types I and II. A breakdown of the number of events per SN type is available in Table 3 in Appendix A.

For all of our events of interest in Lasair 1.0 (Query VI), we find that the vast majority (95.09%) of classified events are SNe, 2.23% (five events) are TDEs, 0.45% are BFFs, and 0.89% are flaring AGNs.<sup>20</sup> The remaining 1.34% consist of one

<sup>20</sup> Here, the term “flaring AGN” refers to events with coherent brightening episodes much stronger than any typical variability seen in their historical light curves. Specifically, the flares seen here rose by 0.25 magnitudes on average in one week, which is much higher than normal AGN variability (e.g., MacLeod et al. 2012; Caplar et al. 2017).

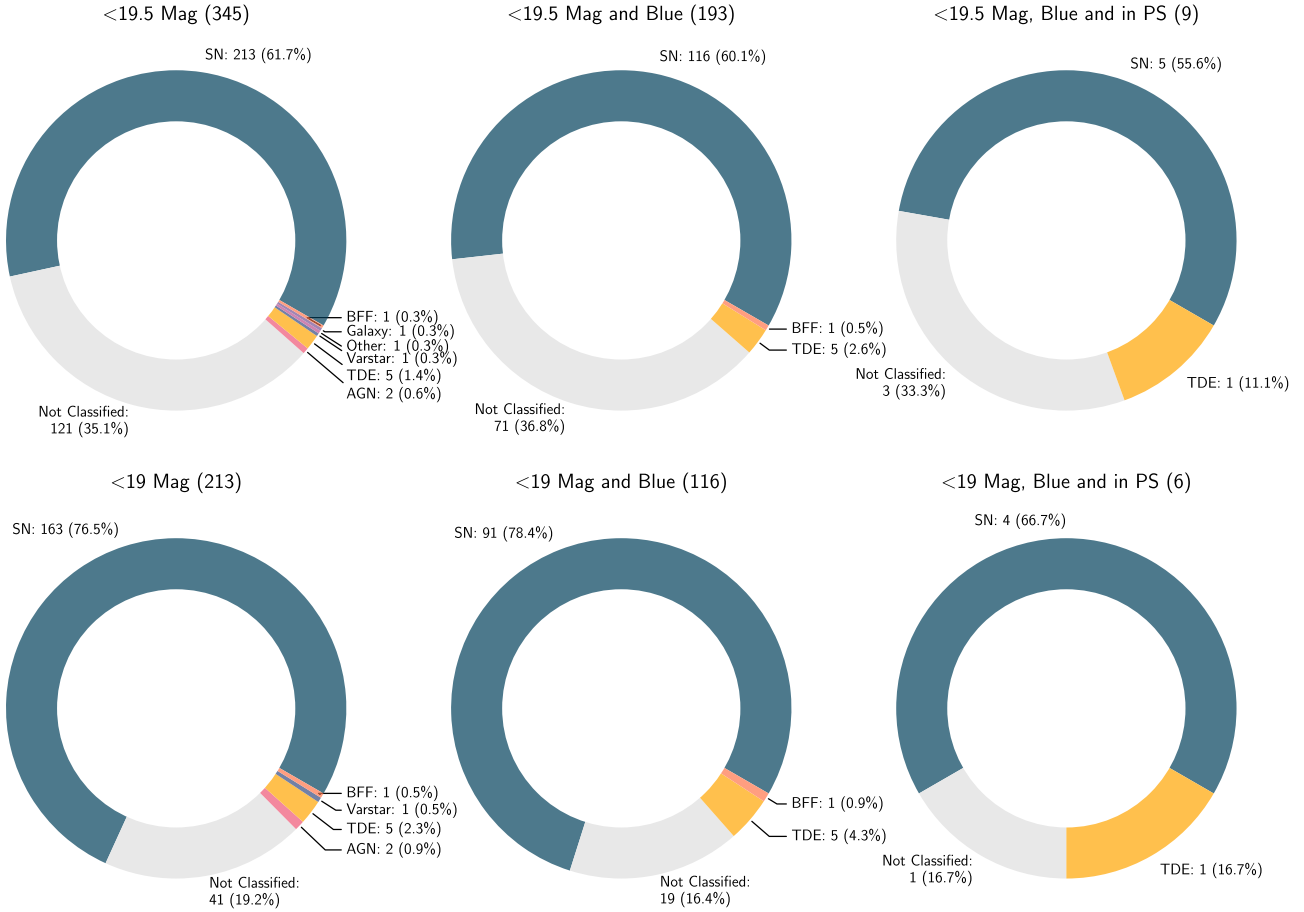


**Figure 2.** Numbers and fractions of the classes of candidates of interest from the different Lasair 1.0 queries, as detailed in the text and in Table 1. The numbers in parentheses next to each subplot title denote the total number of events in that query.

variable star, one event classified as “Galaxy” (which means that it was either an artifact or it faded before the spectrum was obtained), and one classified as “Other.” The “Other” event is AT 2022amc, which displays a featureless blue continuum. This could have been a young core-collapse SN or some other hot flare, including an SMBH-related one, such as a TDE or BFF. Unfortunately, no follow-up spectra were posted to TNS or, to our knowledge, published elsewhere, so its nature remains undetermined.

The five TDEs are AT 2020vwl (ZTF20achpcvt, also named ATLAS20bdgk and Gaia20etp; Hammerstein et al. 2021), AT 2021ehb (ZTF21aanxhjv, also named ATLAS21jdy; Alexander et al. 2021; Gezari et al. 2021; Yao 2021, 2022), AT 2022bdw (ZTF22aahtqz, also named ATLAS22dth, Gaia22baj, and PS22avi; Arcavi et al. 2022a, 2022b), AT 2022csn (ZTF22aabimec, also named ATLAS22ggz, Gaia22ayp, and PS22bju; Arcavi & Pellegrino 2022), and AT 2022dbl (ZTF18aabdjajx, also named ASASSN-22ci; Arcavi et al. 2022d; Sfaradi et al. 2022). AT 2020vwl was classified as a “TDE H+He” (van Velzen et al. 2020) by the ZTF group, with a spectrum obtained from the Spectral Energy Distribution Machine (SEDM; Blagorodnova et al. 2018) on the Palomar 60 inch telescope (Cenko et al. 2006). Despite the low spectral resolution, broad He II and H $\alpha$  can be clearly identified, on top of a blue continuum, making the TDE classification secure. AT 2021ehb was also classified by the ZTF team using an SEDM spectrum, but that spectrum is not publicly available on the TNS. Follow-up spectra that are

available on the TNS do not show clear TDE signatures, but X-ray detections (Yao et al. 2021) make the TDE classification likely. AT 2022bdw, AT 2022csn, and AT 2022dbl were classified by the effort presented here, using the Las Cumbres Observatory Floyds spectrographs, based on broad H and He II spectral features on top of a blue continuum. AT 2022csn was initially classified by the ePESSTO+ collaboration as a Type I SLSN (Srivastav et al. 2022a, 2022b), but later reclassified by us as a TDE after the emergence of TDE spectral features. AT 2022dbl is also listed on the TNS as AT 2018mac, due to a sporadic detection in 2018 at a similar position, likely resulting from an image-subtraction artifact. This is the only TDE out of the five found in a PS host from the French & Zabludoff (2018) catalog. We conclude that all five TDE classifications are secure, with the possible exception of AT 2021ehb, since its classification spectrum is not available on the TNS.

The BFF is AT 2021seu (ZTF21abjciua, also named ATLAS21bbfi; Arcavi et al. 2021), also classified by this effort using Floyds (Arcavi 2021). The classification is based on a possible N III/He II emission complex on top of a blue continuum, not seen in an archival SDSS spectrum at that position (Arcavi et al. 2021), and resembling the spectra of BFFs in Trakhtenbrot et al. (2019).

All five TDEs pass the “blue criterion” (Criterion 11) and were found by Query V, but the number of SNe passing this criterion is much smaller, nearly doubling the percentage of TDEs among classified blue transients. Limiting the search to candidates that are both blue and brighter than magnitude 19 at

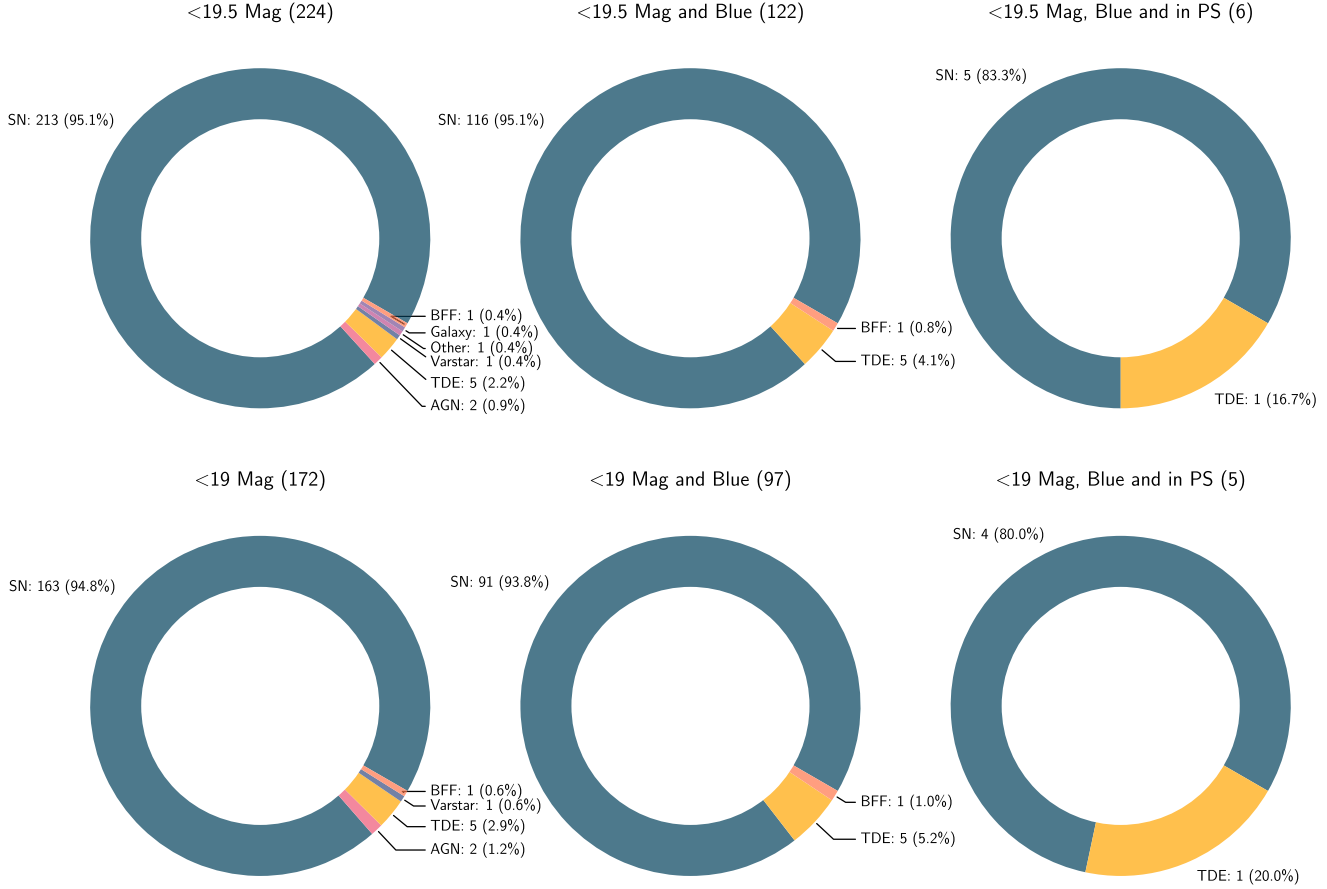


**Figure 3.** The same as Figure 2, but for classified events only.

**Table 2**  
Fractions of Classified Candidates of Interest from the Different Queries with  $1\sigma$  Clopper–Pearson Confidence Bounds

Query	SN	AGN	TDE	Other	Galaxy	BFF	Varstar
I	$80.00\% \pm 17.79\%$	0	$20.00\% \pm 17.79\%$	0	0	0	0
II	$93.81\% \pm 2.43\%$	0	$5.15\% \pm 2.23\%$	0	$1.03\% \pm 1.02\%$	0	0
III	$94.77\% \pm 1.69\%$	$1.16\% \pm 0.81\%$	$2.91\% \pm 1.27\%$	$0.58\% \pm 0.58\%$	$0.58\% \pm 0.58\%$	0	0
IV	$83.33\% \pm 15.13\%$	0	$16.67\% \pm 15.13\%$	0	0	0	0
V	$95.08\% \pm 1.95\%$	0	$4.10\% \pm 1.78\%$	0	$0.82\% \pm 0.81\%$	0	0
VI	$95.09\% \pm 1.44\%$	$0.89\% \pm 0.63\%$	$2.23\% \pm 0.98\%$	$0.45\% \pm 0.44\%$	$0.45\% \pm 0.44\%$	$0.45\% \pm 0.44\%$	$0.45\% \pm 0.44\%$
VII	$70.00\% \pm 10.19\%$	$30.00\% \pm 10.19\%$	0	0	0	0	0
VIII	$72.73\% \pm 9.44\%$	$27.27\% \pm 9.44\%$	0	0	0	0	0
IX	0	$100.00\% \pm 0.00\%$	0	0	0	0	0
X	0	$100.00\% \pm 0.00\%$	0	0	0	0	0

discovery (Query II) keeps all TDEs and further increases their percentage to 5.15%. Looking at events in PS galaxies (Query IV),<sup>21</sup> only one of the five TDEs remains, but it is one of six (16.67%) classified transients there. This is consistent (to  $1.2\sigma$ ) with the finding of Arcavi et al. (2022c) that  $10.0\% \pm 5.5\%$  of classified transients in PS galaxies should be TDEs.

For all of our events of interest in Lasair 3.0 (Query VIII), SNe are still the majority of classified events (72.73%), with the rest all flaring AGNs. The fraction of flaring AGNs in Lasair 3.0 is thus 30 times larger than in Lasair 1.0. Some of this difference is likely explained by the fact that, at least

initially, Lasair 3.0 did not provide the full multiyear light-curve history of each candidate. This precluded filtering most AGNs by their historical activity.

In order to quantify the significance of the difference in fractions between queries, we calculate their confidence bounds using the Clopper–Pearson method (Clopper & Pearson 1934). Gehrels (1986) discusses how this method, which uses binomial statistics to estimate lower and upper confidence bounds for ratios, is especially useful for ratios of different event types, when the numbers of observed events are small. The  $1\sigma$  confidence bounds calculated with this method (and used hereafter) are shown in Table 2.

The fraction of TDEs in our global Lasair 1.0 query (Query VI) is  $2.23\% \pm 0.98\%$  and that of BFFs is  $0.45\% \pm 0.44\%$ .

<sup>21</sup> Here, we study all events that were both in a PS host and blue. There were two more transients in PS hosts that were not blue: ZTF20acselm (a Type Ia SN) and ZTF22aabsemf (an unclassified event).

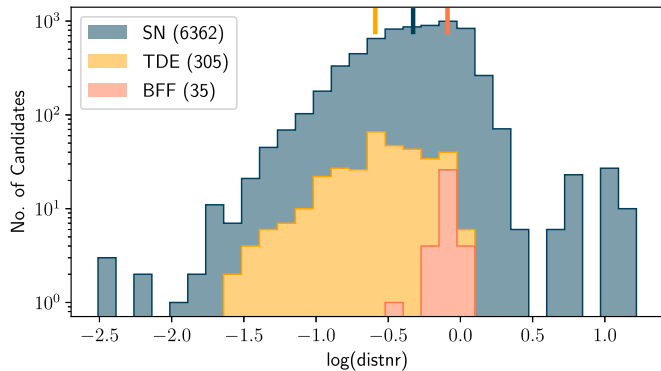


**Figure 4.** Distribution of the `distnr` parameter, which quantifies the offset of a source from its host galaxy center (shown in a stacked histogram) for all detections of SNe, TDEs, and the BFF. The vertical lines at the top denote the average value for each class. The number of total detections per class of events is shown in parentheses in the legend. While TDEs show a lower average offset compared to SNe, the difference is not large enough to be used a discriminant.

Requiring candidates to be blue (Query V) increases the TDE fraction by a factor of  $1.84 \pm 1.11$ . Adding the requirement for a PS host (Query IV) increases the TDE fraction by a factor of  $7.47 \pm 7.53$  compared to the global query (Query VI). Without the full light-curve history of Lasair 3.0, the fraction of AGNs there increases by a factor of  $30.55 \pm 23.86$  in Query VIII compared to Query VI.

We wish to check whether the offset of a source from its host galaxy center can be used as a way to better select for TDEs and BFFs. To do that, we retrieved the `distnr` parameter of each detection of each SN, TDE, and the BFF in our sample using the Automatic Learning for the Rapid Classification of Events (ALeRCE) broker<sup>22</sup> (Förster et al. 2021). The `distnr` parameter is provided with each detection of a source in the ZTF alert packets.<sup>23</sup> It denotes the distance of that detection to the nearest source in the reference-image PSF catalog (within  $30''$ ), in units of pixels (which are equal to units of  $''$ , since the ZTF pixel scale is 1 pixel per  $''$ ). We plot the distribution of these values in Figure 4. TDEs show a slightly lower average `distnr` value than SNe, but the difference is much smaller than the spread of values of each type of event and hence not significant. Our one BFF actually shows a larger average `distnr` value than the SNe. However, this is based on detections of a single event, and could be driven by the centroid measurement of its particular host galaxy in ZTF. We conclude that there is no significant difference in the `distnr` values between SNe, TDEs, and BFFs in ZTF, and therefore that this parameter is not a good discriminant.

There are 24 additional events that are classified as TDEs on the TNS, from the time period of our search, which do not appear here. Of those, 16 have robust TDE classifications (i.e., at least one public spectrum showing clear broad He II and/or H $\alpha$  emission and blue colors). The rest have either no public spectrum available, very noisy spectra, or show no clear spectral features. Of the 16 robust TDEs, most (11) have not been identified here because they were deemed not to have a coherent rising light curve at discovery. Three events were missed due to a bug in the queries (which was later fixed), and two did not pass Criterion 7, regarding the number of unreliable detections (one required increasing the number of unreliable

detections from  $<3$  to  $<5$ , and one required it to be increased to  $<21$ ). However, relaxing Criterion 7 would have likely also led to an increase in contaminant candidates.

#### 4. Discussion and Conclusions

Our results quantify the “needle in a haystack” problem of finding TDEs and BFFs in wide-field transient surveys. We find that the photometric history of candidates is crucial for removing most AGN contamination. Even so, roughly one in 35–45 events is a TDE, and one in 170–220 is a BFF. This sets a significant challenge for identifying these events in current transient surveys, and for identifying even a small subset of the thousands of TDEs expected to be discovered by the Legacy Survey of Space and Time (LSST; Ivezić et al. 2019) every year (Bricman & Gomboc 2020).

The fraction of TDEs increases by almost a factor of 2 to roughly one in 20–25 events when selecting only blue ( $g - r < 0.05$ ) transients. This cut does not remove any TDEs. The fraction further increases by another factor of  $\sim 3$  to roughly one in 5–6 events when selecting probable TDE host galaxies. However, such galaxies are rare, making the total number of TDEs discoverable in this way small. Given the huge increase in expected TDE discovery fractions, though, it would be beneficial to update the French & Zabludoff (2018) galaxy catalog and to expand its coverage using new spectroscopic and photometric surveys such as SDSS-V (Kollmeier et al. 2017).

An additional  $\sim 50\%$  of TDEs are found when relaxing Criterion 7 to allow events with a smaller number of reliable detections, and roughly three times as many TDEs are found when relaxing the condition that the event be rising in brightness at discovery. However, the number of contaminants that relaxing such criteria adds is significant. For example, changing the threshold of Criterion 7 from  $<3$  to  $<5$  (which would have added one TDE to the sample) increased the number of daily candidates by a factor of 2–3, and changing it to  $<21$  (which would have added a second TDE to the sample) increased the number of daily candidates by an order of magnitude.

We find no significant difference between the offsets of TDEs versus nuclear SNe from their host galaxy centers. Therefore, this parameter cannot be used as a discriminant for selecting more likely TDEs, at least not in ZTF, as quantified by the `distnr` parameter. LSST, with its higher spatial resolution, might be able to make host nucleus offsets a more viable distinguishing parameter.

An additional possible discriminant for selecting TDEs, which was not tested here, is their ultraviolet to optical colors (e.g., Hung et al. 2018). Obtaining ultraviolet photometry rapidly and for many targets is currently possible almost exclusively with the the Neil Gehrels Swift Observatory (Gehrels et al. 2004) Ultraviolet/Optical Telescope (Roming et al. 2005). Indeed, Hung et al. (2018) have shown that selecting transients by a combination of their ultraviolet to optical colors using Swift and the optical colors of their host galaxies increased the fraction of TDEs to one in 4.5. However, Swift is limited in the number of transients it can vet. The upcoming Ultraviolet Transient Astronomy Satellite (Sagiv et al. 2014), with its wide-field ultraviolet imager, is expected to obtain ultraviolet photometry for thousands of TDEs. This will be an excellent way to discriminate TDEs from other

<sup>22</sup> <https://alerce.science/>

<sup>23</sup> <https://zwickytransientfacility.github.io/ztf-avro-alert/schema.html>

transients without the need for substantial classification resources.

Another approach is to train machine-learning algorithms to classify transients from photometry alone. This has been done for distinguishing between some SN types (e.g., Richards et al. 2012; Möller et al. 2016; Charnock & Moss 2017; Boone 2019; Ishida et al. 2019; Villar et al. 2019, 2020; Gomez et al. 2020; Hosseinzadeh et al. 2020). Until recently, the number of observed TDEs has been too small to be used for classification training, leading Muthukrishna et al. (2019) to train their algorithm on simulated TDE light curves. Today, with TDE light curves available for dozens of events, it might be possible to effectively train a machine-learning algorithm to distinguish TDE light curves from those of other SNe. How effectively this can be done, and at what phase of the light curve a robust classification can be obtained (if at all), remains to be tested.

Of course, any such filtering based on the photometric properties of the transient or the characteristics of its host galaxy can also bias population studies of TDEs and BFFs. A specific population that almost all current searches (including ours) are biased against is that of slowly evolving transients with years-long evolution. Such events are already suppressed by the alert mechanisms of most transient surveys, even before reaching the brokers. ZTF alerts, for example, are generated by comparing a new image to a reference image taken up to a few months to a few years earlier. Therefore, events that rise on a timescale of several years will not be much brighter in the new image compared to the reference, and thus an alert might never be issued. Since the set of images used as references is updated from time to time, such transients could remain hidden during the lifetimes of the surveys. Indeed, when Lawrence et al. (2016) compared images from PS1 to images obtained a decade earlier by SDSS, they found a population of slowly rising nuclear transients. This population is not seen in current transient surveys, which are optimized to find transients that change on shorter timescales.

It will thus continue to be challenging to find TDEs and BFFs in optical transient surveys in an unbiased way, even for events evolving on timescales of days to months. One way forward is to use some combination of well-defined photometric and host galaxy filters, such as those used here.

However, making searches as complete as possible will still require ample spectroscopic resources for vetting large numbers of SMBH-related transient candidates.

## Acknowledgments

We thank B. Trakhtenbrot for providing some of the spectroscopy time on the Las Cumbres network used to classify candidates identified here, and A. Lawrence, K. Smith, R. Williams, and D. Young for assistance with using Lasair and for helpful comments. We also thank M. Nicholl for implementing many of the queries used here on Lasair, as well as the French & Zabludoff (2018) galaxy catalog as a watchlist there, and A. Riba for developing a Target and Observation Manager used to manually inspect candidates and schedule follow-up observations. We are grateful to B. Zackay for helpful comments regarding host offsets.

Y.D., I.A., and L.M. acknowledge support from the European Research Council (ERC) under the European Union’s Horizon 2020 research and innovation program (grant agreement number 852097). I.A. is a CIFAR Azrieli Global Scholar in the Gravity and the Extreme Universe Program and acknowledges support from that program, from the Israel Science Foundation (grant No. 2752/19), from the United States-Israel Binational Science Foundation (BSF; grant No. 2018166), and from the Israeli Council for Higher Education Alon Fellowship. This work makes use of observations with the Las Cumbres Observatory global telescope network. The Las Cumbres Observatory group is supported by NSF grants AST-1911151 and AST-1911225 and BSF grant 2018166.

## Appendix A Fractions of SN Subtypes

We list the division of SN types found by each query in Table 3. The majority of contaminants across all queries are Type Ia SNe, with the next most likely contaminant being Type II SNe (including their subvariants IIb and IIn). The ZTF Bright Transient Survey (BTS; Perley et al. 2020) aims to classify all transients brighter than certain magnitude cuts (similar to our Query III), but, unlike this work, does not focus on galaxy nuclei. Their Type Ia SN fraction is lower than ours

**Table 3**  
Internal Division of SN Types from the Different Queries

Query	Total SNe	SN Ia	SN Ib	SN Ic	SN Ic-BL	SN I	SN II	SN IIb	SN IIn	SN	SLSN
I	4	4 (100.0%)	0	0	0	0	0	0	0	0	0
II	91	76 (83.5%)	1 (1.1%)	0	2 (2.2%)	0	10 (11.0%)	0	2 (2.2%)	0	0
III	163	134 (82.2%)	2 (1.2%)	2 (1.2%)	4 (2.5%)	0	17 (10.4%)	0	3 (1.8%)	1 (0.6%)	0
IV	5	5 (100.0%)	0	0	0	0	0	0	0	0	0
V	116	97 (83.6%)	1 (0.9%)	0	2 (1.7%)	0	13 (11.2%)	0	2 (1.7%)	0	1 (0.9%)
VI	213	175 (82.2%)	2 (0.9%)	3 (1.4%)	4 (1.9%)	1 (0.5%)	21 (9.9%)	1 (0.5%)	3 (1.4%)	1 (0.5%)	2 (0.9%)
VII	14	8 (57.1%)	0	0	0	0	4 (28.6%)	0	2 (14.3%)	0	0
VIII	16	10 (62.5%)	0	0	0	0	4 (25.0%)	0	2 (12.5%)	0	0
IX	0	0	0	0	0	0	0	0	0	0	0
X	0	0	0	0	0	0	0	0	0	0	0

( $\sim 73\%$  versus  $\sim 82\%$  here) and their Type II SN fraction is higher ( $\sim 20\%$  versus  $\sim 10\%$  here).<sup>24</sup> Since Type Ia and Type II SNe have similar radial distributions in their host galaxies (e.g., Prieto et al. 2008), this difference might be a selection effect, whereby Type Ia SNe are preferentially detected in this work compared to the BTS, since they are more luminous than Type II events and stand out more clearly in bright galaxy nuclei. As found previously by Arcavi et al. (2022c), Type Ia SNe are the only contaminant of TDEs and BFFs in PS galaxies (unless AGNs cannot be fully filtered out, as in the case of the Lasair 3.0 queries).

## Appendix B Results per Separation Threshold

As mentioned in Section 2, we split the Lasair 1.0 sample into two subsamples, each with a different separation threshold for Condition 1 ( $0.^{\prime\prime}5$  and  $1.^{\prime\prime}$ ). The fractions (Table 1) of the split per separation threshold are presented in Table 4 (for the  $0.^{\prime\prime}5$  threshold) and Table 5 (for the  $1.^{\prime\prime}$  threshold).

In order to assess if there is a statistically significant difference between the fractions resulting from the different thresholds, we calculate the  $1\sigma$  Clopper–Pearson confidence bounds per each separation threshold subsample in Table 6 (for the  $0.^{\prime\prime}5$  threshold) and Table 7 (for the  $1.^{\prime\prime}$  threshold).

There are no statistically significant differences between the results of the two separation thresholds. It does appear that there is a much higher fraction of TDEs in the subsample of the  $1.^{\prime\prime}$  threshold (of order 10%) compared to the  $0.^{\prime\prime}5$  threshold (of order 1%). However, this is not statistically significant and is a

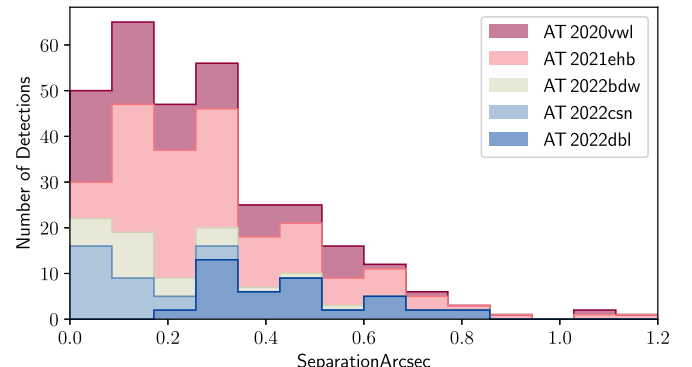


**Figure 5.** Distribution of the `separationArcsec` parameter from Criterion 1 (shown in a stacked histogram) for all detections of our five TDEs. There is no significant difference in the separations between the TDEs in the  $0.^{\prime\prime}5$  threshold subsample (AT 2020vwl and AT 2021ehb) and the TDEs in the  $1.^{\prime\prime}$  threshold subsample (AT 2022bdw, AT 2022csn, and AT 2022dbl), meaning that the change of separation threshold does not have a strong effect on the number of TDEs discovered.

result of small number statistics. To demonstrate this, we plot all of the `separationArcsec` values of all the detections of our five TDEs in Figure 5.

Most detections for the two TDEs in the  $0.^{\prime\prime}5$  threshold subsample and the three TDEs in the  $1.^{\prime\prime}$  threshold subsample are below  $0.^{\prime\prime}5$  separation. This means that the increase of the threshold to  $1.^{\prime\prime}$  is not responsible for the larger fraction of TDEs in that subsample, but rather it is a small number statistics fluctuation.

**Table 4**  
The Same as Table 1, but Only for Events in Lasair 1.0 Selected with a Separation (Condition 1) Threshold of  $0.^{\prime\prime}5$

Query	Total Transients	Not Classified	SN	AGN	TDE	Other	Galaxy	BFF	Varstar
Lasair 1.0									
I: $<19$ Mag, Blue, and in PS	4	1	3	0	0	0	0	0	0
Percentage of All Transients	...	25.00%	75.00%	0	0	0	0	0	0
Percentage of Classified Transients	...	...	100.00%	0	0	0	0	0	0
II: $<19$ Mag and Blue	96	17	76	0	2	0	1	0	0
Percentage of All Transients	...	17.71%	79.17%	0	2.08%	0	1.04%	0	0
Percentage of Classified Transients	...	...	96.20%	0	2.53%	0	1.27%	0	0
III: $<19$ Mag	186	38	143	1	2	1	1	0	0
Percentage of All Transients	...	20.43%	76.88%	0.54%	1.08%	0.54%	0.54%	0	0
Percentage of Classified Transients	...	...	96.62%	0.68%	1.35%	0.68%	0.68%	0	0
IV: $<19.5$ Mag, Blue, and in PS	7	3	4	0	0	0	0	0	0
Percentage of All Transients	...	42.86%	57.14%	0	0	0	0	0	0
Percentage of Classified Transients	...	...	100.00%	0	0	0	0	0	0
V: $<19.5$ Mag and Blue	169	67	99	0	2	0	1	0	0
Percentage of All Transients	...	39.64%	58.58%	0	1.18%	0	0.59%	0	0
Percentage of Classified Transients	...	...	97.06%	0	1.96%	0	0.98%	0	0
VI: $<19.5$ Mag	310	113	191	1	2	1	1	1	0
Percentage of All Transients	...	36.45%	61.61%	0.32%	0.65%	0.32%	0.32%	0.32%	0
Percentage of Classified Transients	...	...	96.95%	0.51%	1.02%	0.51%	0.51%	0.51%	0

<sup>24</sup> <https://sites.astro.caltech.edu/ztf/bts/bts.php>

**Table 5**  
The Same as Table 1, but Only for Events in Lasair 1.0 Selected with a Separation (Condition 1) Threshold of 1"

Query	Total Transients	Not Classified	SN	AGN	TDE	Other	Galaxy	BFF	Varstar
Lasair 1.0									
I: <19 Mag, Blue, and in PS	2	0	1	0	1	0	0	0	0
Percentage of All Transients	...	0	50.00%	0	50.00%	0	0	0	0
Percentage of Classified Transients	...	...	50.00%	0	50.00%	0	0	0	0
II: <19 Mag and Blue	20	2	15	0	3	0	0	0	0
Percentage of All Transients	...	10.00%	75.00%	0	15.00%	0	0	0	0
Percentage of Classified Transients	...	...	83.33%	0	16.67%	0	0	0	0
III: <19 Mag	27	3	20	1	3	0	0	0	0
Percentage of All Transients	...	11.11%	74.07%	3.70%	11.11%	0	0	0	0
Percentage of Classified Transients	...	...	83.33%	4.17%	12.50%	0	0	0	0
IV: <19.5 Mag, Blue, and in PS	2	0	1	0	1	0	0	0	0
Percentage of All Transients	...	0	50.00%	0	50.00%	0	0	0	0
Percentage of Classified Transients	...	...	50.00%	0	50.00%	0	0	0	0
V: <19.5 Mag and Blue	24	4	17	0	3	0	0	0	0
Percentage of All Transients	...	16.67%	70.83%	0	12.50%	0	0	0	0
Percentage of Classified Transients	...	...	85.00%	0	15.00%	0	0	0	0
VI: <19.5 Mag	35	8	22	1	3	0	0	0	1
Percentage of All Transients	...	22.86%	62.86%	2.86%	8.57%	0	0	0	2.86%
Percentage of Classified Transients	...	...	81.48%	3.70%	11.11%	0	0	0	3.70%

**Table 6**  
The Same as Table 2, but Only for Events in Lasair 1.0 Selected with a Separation (Condition 1) Threshold of 0.5"

Query	SN	AGN	TDE	Other	Galaxy	BFF	Varstar
I	100.00% $\pm$ 0.00%	0	0	0	0	0	0
II	96.20% $\pm$ 2.14%	0	2.53% $\pm$ 1.76%	0	1.27% $\pm$ 1.25%	0	0
III	96.62% $\pm$ 1.48%	0.68% $\pm$ 0.67%	1.35% $\pm$ 0.94%	0.68% $\pm$ 0.67%	0.68% $\pm$ 0.67%	0	0
IV	100.00% $\pm$ 0.00%	0	0	0	0	0	0
V	97.06% $\pm$ 1.66%	0	1.96% $\pm$ 1.37%	0	0.98% $\pm$ 0.97%	0	0
VI	96.95% $\pm$ 1.22%	0.51% $\pm$ 0.50%	1.02% $\pm$ 0.71%	0.51% $\pm$ 0.50%	0.51% $\pm$ 0.50%	0.51% $\pm$ 0.50%	0

**Table 7**  
The Same as Table 2, but Only for Events in Lasair 1.0 Selected with a Separation (Condition 1) Threshold of 1"

Query	SN	AGN	TDE	Other	Galaxy	BFF	Varstar
I	50.00% $\pm$ 35.16%	0	50.00% $\pm$ 35.16%	0	0	0	0
II	83.33% $\pm$ 8.74%	0	16.67% $\pm$ 8.74%	0	0	0	0
III	83.33% $\pm$ 7.57%	4.17% $\pm$ 4.06%	12.50% $\pm$ 6.71%	0	0	0	0
IV	50.00% $\pm$ 35.16%	0	50.00% $\pm$ 35.16%	0	0	0	0
V	85.00% $\pm$ 7.94%	0	15.00% $\pm$ 7.94%	0	0	0	0
VI	81.48% $\pm$ 7.43%	3.70% $\pm$ 3.61%	11.11% $\pm$ 6.01%	0	0	0	3.70% $\pm$ 3.61%

## Appendix C List of Events

We list in Table 8 the full set of events considered transients of interest in this work, their publicly available classification and redshift, and the query number(s) in which they were found.

**Table 8**  
Candidates of Interest

ZTF Name	TNS Name	Other Names	R.A. (deg)	Decl. (deg)	Query	Classification	Redshift	Note	Reference(s)
ZTF18aabdajx	AT 2022dbl (also AT 2018mac)	ASASSN-22ci	185.1878	49.55128	I	TDE	0.0284		Arcavi et al. (2022d), Sfaradi et al. (2022)
ZTF18aacnlxz	SN 2020aavr	...	134.95468	38.10909	III	SN II	0.072475		Burke et al. (2020b)
ZTF18aadsuxd	AT 2020yui	ATLAS20bfc, PS20kyb, ZTF18aaefvaq	129.53396	31.66792	III	...	...		...
ZTF18aagtwyh	SN 2021oud	Gaia21cyq, ZTF18ahbypm	189.92466	16.53793	II	SN Ia	0.066041		SNIascore (2021a)
ZTF18aahfbqp	SN 2020acua	...	156.67845	21.7239	III	SN Ia	0.041362		Hiramatsu et al. (2020a)

**Notes.** Since some queries are subsets of other queries, here we list only the most stringent query that produced each event.

<sup>a</sup> Not clear if it is indeed rising at discovery.

<sup>b</sup> Lower than the expected signal-to-noise ratio in the spectrum attempt.

<sup>c</sup> Faded before the spectrum was attempted (could have been rapidly evolving or an artifact).

(This table is available in its entirety in machine-readable form.)

## ORCID iDs

Yael Dgany <https://orcid.org/0000-0002-7579-1105>  
 Iair Arcavi <https://orcid.org/0000-0001-7090-4898>  
 Lydia Makrygianni <https://orcid.org/0000-0002-7466-4868>  
 Craig Pellegrino <https://orcid.org/0000-0002-7472-1279>  
 D. Andrew Howell <https://orcid.org/0000-0003-4253-656X>

## References

Aamer, A., O'Neill, D., Killestein, T., et al. 2022c, TNSAN, **48**, 1  
 Aamer, A., O'Neill, D., Ridley, E., et al. 2022a, TNSCR, **2022-291**, 1  
 Aamer, A., Ridley, E., O'Neill, D., et al. 2022b, TNSAN, **29**, 1  
 Alam, S., Albareti, F. D., Allende Prieto, C., et al. 2015, *ApJS*, **219**, 12  
 Alexander, K. D., Goodwin, A. J., Miller-Jones, J., et al. 2021, TNSAN, **309**, 1  
 Anderson, J., Pessi, P., Galbany, L., et al. 2020, TNSAN, **244**, 1  
 Angus, C. 2021, TNSCR, **2021-1179**, 1  
 Arcavi, I. 2021, TNSCR, **2021-2460**, 1  
 Arcavi, I., & Dgany, Y. 2023, TNSCR, **2023-853**, 1  
 Arcavi, I., Dgany, Y., & Pellegrino, C. 2022a, TNSAN, **50**, 1  
 Arcavi, I., Dgany, Y., Pellegrino, C., et al. 2022b, TNSCR, **2022-511**, 1  
 Arcavi, I., Dgany, Y., Pellegrino, C., et al. 2022d, TNSCR, **2022-504**, 1  
 Arcavi, I., Dgany, Y., Trakhtenbrot, B., et al. 2022e, TNSCR, **2022-512**, 1  
 Arcavi, I., Gal-Yam, A., Sullivan, M., et al. 2014, *ApJ*, **793**, 38  
 Arcavi, I., Newsome, M., Dgany, Y., et al. 2021, TNSAN, **195**, 1  
 Arcavi, I., Nyiha, I., & French, K. D. 2022c, *ApJ*, **924**, 121  
 Arcavi, I., & Pellegrino, C. 2022, TNSCR, **2022-3660**, 1  
 Balam, D. D., & Kendurkar, M. 2022, TNSAN, **37**, 1  
 Balcon, C. 2021, TNSCR, **2021-1047**, 1  
 Bellm, E. 2014, in The Third Hot-wiring the Transient Universe Workshop, ed. P. R. Wozniak et al., **27**  
 Blagorodnova, N., Cenko, S. B., Kulkarni, S. R., et al. 2019, *ApJ*, **873**, 92  
 Blagorodnova, N., Neill, J. D., Walters, R., et al. 2018, *PASP*, **130**, 035003  
 Boone, K. 2019, *AJ*, **158**, 257  
 Bowen, I. S. 1928, *ApJ*, **67**, 1  
 Bricman, K., & Gomboc, A. 2020, *ApJ*, **890**, 73  
 Brown, T. M., Baliber, N., Bianco, F. B., et al. 2013, *PASP*, **125**, 1031  
 Bruch, R., Strotjohann, N., Gal-Yam, A., et al. 2021, TNSAN, **200**, 1  
 Burke, J., Arcavi, I., Hiramatsu, D., et al. 2020a, TNSCR, **2020-3361**, 1  
 Burke, J., Dgani, Y., Arcavi, I., et al. 2020b, TNSCR, **2020-3662**, 1  
 Burke, J., Dgani, Y., & Arcavi, I. 2020c, TNSCR, **2020-3412**, 1  
 Burke, J., Dgani, Y., & Arcavi, I. 2020d, TNSCR, **2020-3499**, 1  
 Burke, J., Dgani, Y., & Arcavi, I. 2020e, TNSCR, **2020-3823**, 1  
 Burke, J., Dgani, Y., & Arcavi, I. 2021a, TNSCR, **2021-36**, 1  
 Burke, J., Dgani, Y., & Arcavi, I. 2021b, TNSCR, **2021-50**, 1  
 Burke, J., Dgani, Y., & Arcavi, I. 2021c, TNSCR, **2021-680**, 1  
 Burke, J., Dgani, Y., & Arcavi, I. 2021d, TNSCR, **2021-3859**, 1  
 Burke, J., Dgani, Y., & Arcavi, I. 2021e, TNSCR, **2021-3923**, 1  
 Burke, J., Dgani, Y., Arcavi, I., et al. 2021f, TNSCR, **2021-2075**, 1  
 Burke, J., Dgani, Y., Arcavi, I., et al. 2021g, TNSCR, **2021-2577**, 1  
 Burke, J., Dgani, Y., Arcavi, I., et al. 2021h, TNSCR, **2021-2591**, 1  
 Burke, J., Dgani, Y., Arcavi, I., et al. 2021i, TNSCR, **2021-3250**, 1  
 Burke, J., Dgani, Y., Arcavi, I., et al. 2021j, TNSCR, **2021-4145**, 1  
 Burke, J., Dgani, Y., Arcavi, I., et al. 2022a, TNSCR, **2022-600**, 1  
 Burke, J., Dgani, Y., Arcavi, I., et al. 2022b, TNSCR, **2022-646**, 1  
 Burke, J., Dgani, Y., Arcavi, I., et al. 2022c, TNSCR, **2022-719**, 1  
 Burke, J., Dgany, Y., Arcavi, I., et al. 2020f, TNSCR, **2020-3626**, 1  
 Burke, J., Dgany, Y., Hiramatsu, D., et al. 2020g, TNSCR, **2020-3963**, 1  
 Buzzoni, B., Delabre, B., Dekker, H., et al. 1984, *Msngr*, **38**, 9  
 Callis, E., Ihane, N., Gromadzki, M., et al. 2020, TNSAN, **222**, 1  
 Caplar, N., Lilly, S. J., & Trakhtenbrot, B. 2017, *ApJ*, **834**, 111  
 Carini, R., Gutierrez, C., & Yaron, O. 2021a, TNSCR, **2021-3519**, 1  
 Carini, R., Gutierrez, C., Elias-Rosa, N., et al. 2021b, TNSAN, **265**, 1  
 Cenko, S. B., Fox, D. B., Moon, D.-S., et al. 2006, *PASP*, **118**, 1396  
 Chambers, K. C., Magnier, E. A., Metcalfe, N., et al. 2016, arXiv:1612.05560  
 Chan, C.-H., Piran, T., Krolik, J. H., & Saban, D. 2019, *ApJ*, **881**, 113  
 Charnock, T., & Moss, A. 2017, *ApJL*, **837**, L28  
 Chu, M., Dahiwale, A., & Fremling, C. 2021a, TNSCR, **2021-2547**, 1  
 Chu, M., Dahiwale, A., & Fremling, C. 2021b, TNSCR, **2021-2623**, 1  
 Chu, M., Dahiwale, A., & Fremling, C. 2021c, TNSCR, **2021-2834**, 1  
 Chu, M., Dahiwale, A., & Fremling, C. 2021d, TNSCR, **2021-2980**, 1  
 Chu, M., Dahiwale, A., & Fremling, C. 2021e, TNSCR, **2021-3202**, 1  
 Chu, M., Dahiwale, A., & Fremling, C. 2021f, TNSCR, **2021-3211**, 1  
 Chu, M., Dahiwale, A., & Fremling, C. 2021g, TNSCR, **2021-3263**, 1  
 Clopper, C. J., & Pearson, E. S. 1934, *Biometrika*, **26**, 404  
 Cosentino, S. P., Evans, C. R., Inserra, C., et al. 2022a, TNSCR, **2022-1409**, 1  
 Cosentino, S. P., Evans, C. R., Parrag, E., et al. 2022b, TNSAN, **116**, 1  
 Dahiwale, A., & Fremling, C. 2020a, TNSCR, **2020-3790**, 1  
 Dahiwale, A., & Fremling, C. 2020b, TNSCR, **2020-3837**, 1  
 Dahiwale, A., & Fremling, C. 2020c, TNSCR, **2020-3859**, 1  
 Dahiwale, A., & Fremling, C. 2020d, TNSCR, **2020-3914**, 1  
 Dahiwale, A., & Fremling, C. 2021a, TNSCR, **2021-38**, 1  
 Dahiwale, A., & Fremling, C. 2021b, TNSCR, **2021-66**, 1  
 Dahiwale, A., & Fremling, C. 2021c, TNSCR, **2021-87**, 1  
 Dahiwale, A., & Fremling, C. 2021d, TNSCR, **2021-193**, 1  
 Dahiwale, A., & Fremling, C. 2021e, TNSCR, **2021-223**, 1  
 Dahiwale, A., & Fremling, C. 2021f, TNSCR, **2021-358**, 1  
 Dahiwale, A., & Fremling, C. 2021g, TNSCR, **2021-405**, 1  
 Dahiwale, A., & Fremling, C. 2021h, TNSCR, **2021-435**, 1  
 Dahiwale, A., & Fremling, C. 2021i, TNSCR, **2021-479**, 1  
 Dahiwale, A., & Fremling, C. 2021j, TNSCR, **2021-512**, 1  
 Dahiwale, A., & Fremling, C. 2021k, TNSCR, **2021-569**, 1  
 Dahiwale, A., & Fremling, C. 2021l, TNSCR, **2021-650**, 1  
 Dahiwale, A., & Fremling, C. 2021m, TNSCR, **2021-665**, 1  
 Dahiwale, A., & Fremling, C. 2021n, TNSCR, **2021-885**, 1  
 Dahiwale, A., & Fremling, C. 2021o, TNSCR, **2021-922**, 1  
 Dahiwale, A., & Fremling, C. 2021p, TNSCR, **2021-965**, 1  
 Dahiwale, A., & Fremling, C. 2021q, TNSCR, **2021-1008**, 1  
 Dahiwale, A., & Fremling, C. 2021r, TNSCR, **2021-1102**, 1  
 Dahiwale, A., & Fremling, C. 2021s, TNSCR, **2021-1147**, 1  
 Dahiwale, A., & Fremling, C. 2021t, TNSCR, **2021-1156**, 1  
 Dahiwale, A., & Fremling, C. 2021u, TNSCR, **2021-1197**, 1  
 Dahiwale, A., & Fremling, C. 2021v, TNSCR, **2021-1234**, 1  
 Dahiwale, A., & Fremling, C. 2021w, TNSCR, **2021-1282**, 1  
 Dahiwale, A., & Fremling, C. 2021x, TNSCR, **2021-1378**, 1  
 Dahiwale, A., & Fremling, C. 2021y, TNSCR, **2021-1482**, 1  
 Dahiwale, A., & Fremling, C. 2021z, TNSCR, **2021-1574**, 1  
 Dahiwale, A., & Fremling, C. 2021aa, TNSCR, **2021-1664**, 1  
 Dahiwale, A., & Fremling, C. 2021ab, TNSCR, **2021-1984**, 1  
 Delgado, M., Galbany, L., González, R., et al. 2021a, TNSAN, **23**, 1  
 Delgado, M., Galbany, L., Gonzalez, R., Munoz, S., & Zimmerman, E. 2021b, TNSCR, **2021-215**, 1  
 Delgado, M., González, R., Muñoz, S., et al. 2021c, TNSAN, **206**, 1  
 Dennefeld, M., Ihane, N., Gromadzki, M., et al. 2022a, TNSAN, **102**, 1  
 Dennefeld, M., Ihane, N., Gromadzki, M., & Yaron, O. 2022b, TNSCR, **2022-1200**, 1  
 Dennefeld, M., Taubenberger, S., Holas, A., et al. 2021a, TNSAN, **126**, 1  
 Dennefeld, M., Taubenberger, S., & Yaron, O. 2021b, TNSCR, **2021-1251**, 1  
 Desai, D. 2022, TNSCR, **2022-658**, 1  
 Dimitriadis, G., & Angus, C. 2021, TNSCR, **2021-1224**, 1  
 Dimitriadis, G., & Foley, R. J. 2021, TNSCR, **2021-434**, 1  
 Filippenko, A. V. 1982, *PASP*, **94**, 715  
 Förster, F., Cabrera-Vives, G., Castillo-Navarrete, E., et al. 2021, *AJ*, **161**, 242  
 French, K. D., Arcavi, I., & Zabludoff, A. 2016, *ApJL*, **818**, L21  
 French, K. D., Arcavi, I., Zabludoff, A. I., et al. 2020a, *ApJ*, **891**, 93  
 French, K. D., Wevers, T., Law-Smith, J., Graur, O., & Zabludoff, A. I. 2020b, *SSRv*, **216**, 32  
 French, K. D., & Zabludoff, A. I. 2018, *ApJ*, **868**, 99  
 Fulton, M., Srivastav, S., Smartt, S. J., et al. 2022, TNSCR, **2022-1253**, 1  
 Gehrels, N. 1986, *ApJ*, **303**, 336  
 Gehrels, N., Chincarini, G., Giommi, P., et al. 2004, *ApJ*, **611**, 1005  
 Gezari, S. 2021, *ARA&A*, **59**, 21  
 Gezari, S., Chornock, R., Rest, A., et al. 2012, *Natur*, **485**, 217  
 Gezari, S., Hammerstein, E., Yao, Y., et al. 2021, TNSAN, **103**, 1  
 Gillanders, J., Srivastav, S., Fulton, M., et al. 2021, TNSCR, **2021-86**, 1  
 Gomez, S., Berger, E., Blanchard, P. K., et al. 2020, *ApJ*, **904**, 74  
 Gomez, S., Blanchard, P., Hiramatsu, D., Berger, E., & Hosseinzadeh, G. 2021, TNSCR, **2021-3822**, 1  
 Gonzalez, E. P., Burke, J., Hiramatsu, D., et al. 2021a, TNSCR, **2021-2575**, 1  
 Gonzalez, E. P., & Dgany, Y. 2021, TNSCR, **2021-268**, 1  
 Gonzalez, E. P., Dgany, Y., Burke, J., et al. 2021b, TNSCR, **2021-3609**, 1  
 Gonzalez, E. P., Dgany, Y., Burke, J., et al. 2021c, TNSCR, **2021-1631**, 1  
 Gonzalez, E. P., Dgany, Y., Burke, J., et al. 2021d, TNSCR, **2021-2576**, 1  
 Gonzalez, E. P., Dgany, Y., Burke, J., et al. 2021e, TNSCR, **2021-2979**, 1  
 Gonzalez, E. P., Dgany, Y., Burke, J., et al. 2021f, TNSCR, **2021-3952**, 1  
 Gonzalez, E. P., Dgany, Y., Burke, J., et al. 2021g, TNSCR, **2021-4017**, 1  
 Gonzalez, E. P., Dgany, Y., Burke, J., et al. 2022, TNSCR, **2022-843**, 1  
 Gonzalez, R., Galbany, L., Munoz, S., Delgado, M., & Irani, I. 2021h, TNSCR, **2021-230**, 1  
 Gonzalez, R., Galbany, L., Munoz, S., Delgado, M., & Yaron, O. 2021i, TNSCR, **2021-259**, 1

González, R., Galbany, L., Muñoz, S., et al. 2021a, TNSAN, [25](#), 1

González, R., Galbany, L., Muñoz, S., et al. 2021b, TNSAN, [29](#), 1

Graham, M. J., Kulkarni, S. R., Bellm, E. C., et al. 2019, *PASP*, [131](#), 078001

Gromadzki, M., Hamanowicz, A., Wyrzykowski, L., et al. 2019, *A&A*, [622](#), L2

Gromadzki, M., Ihane, N., Callis, E., et al. 2020e, TNSAN, [234](#), 1

Gromadzki, M., Ihane, N., Callis, E., Fraser, M., & Irani, I. 2020a, TNSCR, [2020-3382](#), 1

Gromadzki, M., Ihane, N., Callis, E., et al. 2020b, TNSCR, [2020-3360](#), 1

Gromadzki, M., Ihane, N., Callis, E., et al. 2020c, TNSAN, [216](#), 1

Gromadzki, M., Ihane, N., Cartier, R., et al. 2021b, TNSAN, [277](#), 1

Gromadzki, M., Ihane, N., Cartier, R., & Yaron, O. 2021a, TNSCR, [2021-3694](#), 1

Gromadzki, M., Ihane, N., Wevers, T., et al. 2020d, TNSAN, [233](#), 1

Hammerstein, E., Gezari, S., Velzen, S. V., et al. 2021, TNSCR, [2021-159](#), 1

Harvey, L., Prentice, S., Deckers, M., et al. 2021a, TNSAN, [72](#), 1

Harvey, L., Prentice, S., Magee, M., Deckers, M., & Zimmerman, E. 2021b, TNSCR, [2021-563](#), 1

Hills, J. G. 1975, *Natur*, [254](#), 295

Hinds, K., Chu, M., Dahiwale, A., & Fremling, C. 2022, TNSCR, [2022-1387](#), 1

Hinds, K., & Perley, D. 2022, TNSCR, [2022-1445](#), 1

Hinkle, J. 2020, TNSCR, [2020-3689](#), 1

Hinshaw, G., Larson, D., Komatsu, E., et al. 2013, *ApJS*, [208](#), 19

Hiramatsu, D., Dgany, Y., Arcavi, I., et al. 2020a, TNSCR, [2020-3921](#), 1

Hiramatsu, D., Dgany, Y., Arcavi, I., et al. 2020b, TNSCR, [2020-3605](#), 1

Hiramatsu, D., Dgany, Y., Arcavi, I., et al. 2020c, TNSCR, [2020-3713](#), 1

Hiramatsu, D., Dgany, Y., Arcavi, I., et al. 2020d, TNSCR, [2020-3778](#), 1

Hiramatsu, D., Dgany, Y., Arcavi, I., et al. 2020e, TNSCR, [2020-3945](#), 1

Hiramatsu, D., Dgany, Y., Arcavi, I., et al. 2021a, TNSCR, [2021-250](#), 1

Hiramatsu, D., Dgany, Y., Arcavi, I., et al. 2021b, TNSCR, [2021-306](#), 1

Hiramatsu, D., Dgany, Y., Arcavi, I., et al. 2021c, TNSCR, [2021-953](#), 1

Hiramatsu, D., Dgany, Y., Arcavi, I., et al. 2021d, TNSCR, [2021-1305](#), 1

Hiramatsu, D., Dgany, Y., Arcavi, I., et al. 2021e, TNSCR, [2021-1717](#), 1

Hiramatsu, D., Dgany, Y., Arcavi, I., et al. 2021f, TNSCR, [2021-1859](#), 1

Hiramatsu, D., Dgany, Y., Arcavi, I., et al. 2021g, TNSCR, [2021-2287](#), 1

Hiramatsu, D., Dgany, Y., Arcavi, I., et al. 2021h, TNSCR, [2021-2303](#), 1

Hiramatsu, D., Dgany, Y., Arcavi, I., et al. 2021i, TNSCR, [2021-2457](#), 1

Hiramatsu, D., Dgany, Y., Arcavi, I., et al. 2021j, TNSCR, [2021-2504](#), 1

Ho, A. Y. Q., Perley, D. A., Gal-Yam, A., et al. 2023, *ApJ*, [949](#), 120

Hosseinzadeh, G., Dauphin, F., Villar, V. A., et al. 2020, *ApJ*, [905](#), 93

Hung, T. 2021, TNSCR, [2021-2317](#), 1

Hung, T., Gezari, S., Cenko, S. B., et al. 2018, *ApJS*, [238](#), 15

Ihane, N., Gromadzki, M., Callis, E., Fraser, M., & Yaron, O. 2020a, TNSCR, [2020-3524](#), 1

Ihane, N., Gromadzki, M., Cartier, R., et al. 2021d, TNSAN, [275](#), 1

Ihane, N., Gromadzki, M., Cartier, R., et al. 2021c, TNSAN, [274](#), 1

Ihane, N., Gromadzki, M., Cartier, R., & Yaron, O. 2021a, TNSCR, [2021-3661](#), 1

Ihane, N., Gromadzki, M., Cartier, R., & Yaron, O. 2021b, TNSCR, [2021-3674](#), 1

Ihane, N., Gromadzki, M., Wevers, T., & Irani, I. 2020b, TNSCR, [2020-3486](#), 1

Ishida, E. E. O., Beck, R., González-Gaitán, S., et al. 2019, *MNRAS*, [483](#), 2

Ivezić, Ž., Kahn, S. M., Tyson, J. A., et al. 2019, *ApJ*, [873](#), 111

Jacobson-Galan, W. 2021, TNSCR, [2021-3666](#), 1

Jacobson-Galán, W., & Foley, R. 2021, TNSAN, [272](#), 1

Jaeger, T. D. 2021, TNSCR, [2021-1460](#), 1

Johansson, J., Chu, M., Dahiwale, A., & Fremling, C. 2022, TNSCR, [2022-1321](#), 1

Kaiser, N., Burgett, W., Chambers, K., et al. 2010, *Proc. SPIE*, [7733](#), 773020

Kankare, E., Nagao, T., Koivisto, N., et al. 2021b, TNSAN, [84](#), 1

Kankare, E., Nagao, T., Koivisto, N., et al. 2021a, TNSCR, [2021-762](#), 1

Killestein, T., Aamer, A., Fulton, M., et al. 2022a, TNSCR, [2022-474](#), 1

Killestein, T., Aamer, A., Fulton, M., et al. 2022c, TNSAN, [46](#), 1

Killestein, T., O'Neill, D., Aamer, A., et al. 2022b, TNSCR, [2022-500](#), 1

Kollmeier, J. A., Zasowski, G., Rix, H.-W., et al. 2017, arXiv:1711.03234

Lawrence, A., Bruce, A. G., MacLeod, C., et al. 2016, *MNRAS*, [463](#), 296

Leadbeater, R. 2021, TNSCR, [2021-1099](#), 1

Leloudas, G., Dai, L., Arcavi, I., et al. 2019, *ApJ*, [887](#), 218

MacLeod, C. L., Ivezić, Ž., Sesar, B., et al. 2012, *ApJ*, [753](#), 106

Madigan, A.-M., Halle, A., Moody, M., et al. 2018, *ApJ*, [853](#), 141

Magee, M., Terwel, J., Prentice, S., Harvey, L., & Strotjohann, N. L. 2021, TNSCR, [2021-327](#), 1

Makrygianni, L., Dgany, Y., Lam, M., et al. 2021a, TNSAN, [170](#), 1

Makrygianni, L., Dgany, Y., Lam, M., et al. 2021b, TNSCR, [2021-1964](#), 1

Makrygianni, L., Trakhtenbrot, B., Arcavi, I., et al. 2023, *ApJ*, [953](#), 32

Mitra, A., Pessi, P., Wiseman, P., et al. 2021, TNSAN, [110](#), 1

Möller, A., Ruhlmann-Kleider, V., Leloup, C., et al. 2016, *JCAP*, [2016](#), 008

Moore, T., Fulton, M., Srivastav, S., et al. 2022c, TNSAN, [66](#), 1

Moore, T., Fulton, M., Srivastav, S., McCollum, M., & Yaron, O. 2022a, TNSCR, [2022-700](#), 1

Moore, T., Srivastav, S., Smith, K. W., et al. 2022d, TNSAN, [74](#), 1

Moore, T., Srivastav, S., Smith, K. W., Fulton, M., & Yaron, O. 2022b, TNSCR, [2022-763](#), 1

Moran, S., Gonzalez-Gaitán, S., Silvestre, J., et al. 2021a, TNSCR, [2021-679](#), 1

Moran, S., Gonzalez-Gaitán, S., Silvestre, J., et al. 2021b, TNSAN, [81](#), 1

Muñoz, S., Delgado, M., González, R., et al. 2021a, TNSCR, [2021-2619](#), 1

Muñoz, S., Galbany, L., Delgado, M., et al. 2021c, TNSAN, [36](#), 1

Muñoz, S., Galbany, L., Delgado, M., Gonzalez, R., & Yaron, O. 2021b, TNSCR, [2021-287](#), 1

Muthukrishna, D., Narayan, G., Mandel, K. S., Biswas, R., & Hložek, R. 2019, *PASP*, [131](#), 118002

Nascimbeni, V., Tomasella, L., Benetti, S., et al. 2021, TNSAN, [251](#), 1

Netzer, H., Elitzur, M., & Ferland, G. J. 1985, *ApJ*, [299](#), 752

Newsome, M., Dgany, Y., Arcavi, I., et al. 2021a, TNSCR, [2021-2380](#), 1

Newsome, M., Dgany, Y., Arcavi, I., et al. 2021b, TNSCR, [2021-3326](#), 1

Newsome, M., Dgany, Y., Arcavi, I., et al. 2021c, TNSCR, [2021-3360](#), 1

Newsome, M., Dgany, Y., Arcavi, I., et al. 2021d, TNSCR, [2021-3663](#), 1

Newsome, M., Dgany, Y., Arcavi, I., et al. 2021e, TNSCR, [2021-3640](#), 1

Newsome, M., Dgany, Y., Arcavi, I., et al. 2021f, TNSCR, [2021-3724](#), 1

Newsome, M., Dgany, Y., Arcavi, I., et al. 2021g, TNSCR, [2021-4018](#), 1

Newsome, M., Dgany, Y., Arcavi, I., et al. 2021h, TNSCR, [2021-4064](#), 1

Newsome, M., Dgany, Y., Arcavi, I., et al. 2021i, TNSCR, [2021-4071](#), 1

Newsome, M., Dgany, Y., Arcavi, I., et al. 2022a, TNSCR, [2022-1275](#), 1

Newsome, M., Dgany, Y., Arcavi, I., et al. 2022b, TNSCR, [2022-1320](#), 1

Nicholl, M., Ridley, E., Gompertz, B., et al. 2021b, TNSAN, [214](#), 1

Nicholl, M., Ridley, E., Gompertz, B., Galbany, L., & Yaron, O. 2021a, TNSCR, [2021-2710](#), 1

Nicholl, M., Ridley, E. J., Oates, S., et al. 2021c, TNSCR, [2021-1812](#), 1

Nicholl, M., Ridley, E. J., Oates, S., et al. 2021d, TNSCR, [2021-1877](#), 1

Pellegrino, C., Dgany, Y., Arcavi, I., et al. 2021a, TNSCR, [2021-158](#), 1

Pellegrino, C., Dgany, Y., Arcavi, I., et al. 2021b, TNSCR, [2021-204](#), 1

Pellegrino, C., Dgany, Y., Arcavi, I., et al. 2021c, TNSCR, [2021-3508](#), 1

Pellegrino, C., Dgany, Y., Arcavi, I., et al. 2021d, TNSCR, [2021-3736](#), 1

Pellegrino, C., Dgany, Y., Arcavi, I., et al. 2021e, TNSCR, [2021-3748](#), 1

Pellegrino, C., Dgany, Y., Arcavi, I., et al. 2021f, TNSCR, [2021-3922](#), 1

Pellegrino, C., Dgany, Y., Arcavi, I., et al. 2022a, TNSCR, [2022-475](#), 1

Pellegrino, C., Dgany, Y., Arcavi, I., et al. 2022b, TNSCR, [2022-501](#), 1

Pellegrino, C., Dgany, Y., Arcavi, I., et al. 2022c, TNSCR, [2022-509](#), 1

Pellegrino, C., Dgany, Y., Arcavi, I., et al. 2022d, TNSCR, [2022-542](#), 1

Pellegrino, C., Dgany, Y., Arcavi, I., et al. 2022e, TNSCR, [2022-1070](#), 1

Pellegrino, C., Dgany, Y., Burke, J., et al. 2021g, TNSCR, [2021-1046](#), 1

Perez-Fournon, I., Poidevin, F., Angel, C. J., et al. 2021, TNSCR, [2021-1952](#), 1

Perley, D. 2020, TNSCR, [2020-3838](#), 1

Perley, D. 2021a, TNSCR, [2021-849](#), 1

Perley, D. 2021b, TNSCR, [2021-1071](#), 1

Perley, D., Chu, M., Dahiwale, A., & Fremling, C. 2022, TNSCR, [2022-1478](#), 1

Perley, D. A., Fremling, C., Sollerman, J., et al. 2020, *ApJ*, [904](#), 35

Perley, D. A., Lunman, R., Yan, L., et al. 2021, TNSAN, [280](#), 1

Pessi, P., Anderson, J., Gutierrez, C., et al. 2020c, TNSAN, [258](#), 1

Pessi, P., Anderson, J., Gutierrez, C., & Irani, I. 2020a, TNSCR, [2020-3811](#), 1

Pessi, P., Csoernyei, G., Holas, A., et al. 2021g, TNSAN, [118](#), 1

Pessi, P., Galbany, L., Nicholl, M., et al. 2021h, TNSAN, [213](#), 1

Pessi, P., Holas, A., Vogl, C., et al. 2021f, TNSAN, [116](#), 1

Pessi, P., Mitra, A., Floers, A., et al. 2021a, TNSCR, [2021-1155](#), 1

Pessi, P., Mitra, A., Holas, A., et al. 2021b, TNSCR, [2021-1178](#), 1

Pessi, P., Mitra, A., Toy, M., et al. 2021e, TNSAN, [111](#), 1

Pessi, P., Mitra, A., Wiseman, P., Toy, M., & Yaron, O. 2021c, TNSCR, [2021-1066](#), 1

Pessi, P., Mitra, A., Wiseman, P., & Yaron, O. 2021d, TNSCR, [2021-1045](#), 1

Pessi, P., Smith, K., Srivastav, S., Gutierrez, C., & Irani, I. 2020b, TNSCR, [2020-3887](#), 1

Pessi, P., Smith, K. W., Srivastav, S., et al. 2020d, TNSAN, [262](#), 1

Pessi, P. J., Anderson, J., Galbany, L., & Yaron, O. 2020e, TNSCR, [2020-3712](#), 1

Pessi, P. J., Galbany, L., Gromadzki, M., et al. 2021k, TNSAN, [209](#), 1

Pessi, P. J., Galbany, L., & Yaron, O. 2021i, TNSCR, [2021-2696](#), 1

Pessi, P. J., Gromadzki, M., & Strotjohann, N. L. 2021j, TNSCR, [2021-2659](#), 1

Piascik, A. S., Steele, I. A., Bates, S. D., et al. 2014, *Proc. SPIE*, [9147](#), 91478H

Prentice, S., Deckers, M., Terwel, J., et al. 2021a, TNSAN, [61](#), [1](#)  
 Prentice, S., Deckers, M., Terwel, J., Magee, M., & Strotjohann, N. L. 2021b, TNSCR, [2021-446](#), [1](#)  
 Prieto, J. L., Stanek, K. Z., & Beacom, J. F. 2008, *ApJ*, [673](#), [999](#)  
 Ragosta, F., Carini, R., Tartaglia, L., et al. 2021a, TNSAN, [297](#), [1](#)  
 Ragosta, F., Carini, R., Tartaglia, L., & Yaron, O. 2021b, TNSCR, [2021-4027](#), [1](#)  
 Rees, M. J. 1988, *Natur*, [333](#), [523](#)  
 Richards, J. W., Homrighausen, D., Freeman, P. E., Schafer, C. M., & Poznanski, D. 2012, *MNRAS*, [419](#), [1121](#)  
 Ridley, E., Gompertz, B., Nicholl, M., et al. 2021a, TNSAN, [220](#), [1](#)  
 Ridley, E., Gompertz, B., Nicholl, M., Galbany, L., & Yaron, O. 2021b, TNSCR, [2021-2795](#), [1](#)  
 Roming, P. W. A., Kennedy, T. E., Mason, K. O., et al. 2005, *SSRv*, [120](#), [95](#)  
 Sagiv, I., Gal-Yam, A., Ofek, E. O., et al. 2014, *AJ*, [147](#), [79](#)  
 Saxton, R., Komossa, S., Auchettl, K., & Jonker, P. G. 2020, *SSRv*, [216](#), [85](#)  
 Schulze, S. 2022, TNSCR, [2022-1276](#), [1](#)  
 Schulze, S., Chu, M., Dahiwale, A., & Fremling, C. 2022, TNSCR, [2022-1282](#), [1](#)  
 Schulze, S., & Sollerman, J. 2021a, TNSAN, [27](#), [1](#)  
 Schulze, S., & Sollerman, J. 2021b, TNSCR, [2021-244](#), [1](#)  
 Sfaradi, I., Horesh, A., & Fender, R. 2022, TNSAN, [57](#), [1](#)  
 Smartt, S. J., Valenti, S., Fraser, M., et al. 2013, *Msngr*, [154](#), [50](#)  
 Smith, K., Fulton, M., Gillanders, J., & Yaron, O. 2021a, TNSCR, [2021-157](#), [1](#)  
 Smith, K. W., Fulton, M., Gillanders, J., et al. 2021b, TNSAN, [18](#), [1](#)  
 Smith, K. W., Fulton, M., Moore, T., et al. 2022b, TNSAN, [54](#), [1](#)  
 Smith, K. W., Fulton, M., Moore, T., Srivastav, S., & Yaron, O. 2022a, TNSCR, [2022-583](#), [1](#)  
 Smith, K. W., Smartt, S. J., Young, D. R., et al. 2020, *PASP*, [132](#), [085002](#)  
 Smith, K. W., Williams, R. D., Young, D. R., et al. 2019, *RNAAS*, [3](#), [26](#)  
 SNIascore 2021a, TNSCR, [2021-2021](#), [1](#)  
 SNIascore 2021b, TNSCR, [2021-1252](#), [1](#)  
 SNIascore 2021c, TNSCR, [2021-1283](#), [1](#)  
 SNIascore 2021d, TNSCR, [2021-1464](#), [1](#)  
 SNIascore 2021e, TNSCR, [2021-1575](#), [1](#)  
 SNIascore 2021f, TNSCR, [2021-1592](#), [1](#)  
 SNIascore 2021g, TNSCR, [2021-1740](#), [1](#)  
 SNIascore 2021h, TNSCR, [2021-1836](#), [1](#)  
 SNIascore 2021i, TNSCR, [2021-1861](#), [1](#)  
 SNIascore 2021j, TNSCR, [2021-1939](#), [1](#)  
 SNIascore 2021k, TNSCR, [2021-2140](#), [1](#)  
 SNIascore 2021l, TNSCR, [2021-2369](#), [1](#)  
 SNIascore 2021m, TNSCR, [2021-2624](#), [1](#)  
 SNIascore 2021n, TNSCR, [2021-2635](#), [1](#)  
 SNIascore 2021o, TNSCR, [2021-2730](#), [1](#)  
 SNIascore 2021p, TNSCR, [2021-2856](#), [1](#)  
 SNIascore 2021q, TNSCR, [2021-2892](#), [1](#)  
 SNIascore 2021r, TNSCR, [2021-3350](#), [1](#)  
 SNIascore 2021s, TNSCR, [2021-3376](#), [1](#)  
 SNIascore 2021t, TNSCR, [2021-3394](#), [1](#)  
 SNIascore 2021u, TNSCR, [2021-3716](#), [1](#)  
 SNIascore 2021v, TNSCR, [2021-3766](#), [1](#)  
 SNIascore 2021w, TNSCR, [2021-3999](#), [1](#)  
 SNIascore 2022a, TNSCR, [2022-457](#), [1](#)  
 SNIascore 2022b, TNSCR, [2022-571](#), [1](#)  
 SNIascore 2022c, TNSCR, [2022-1432](#), [1](#)  
 SNIascore 2022d, TNSCR, [2022-1518](#), [1](#)  
 SNIascore 2022e, TNSCR, [2022-1605](#), [1](#)  
 Sollerman, J., Chu, M., Dahiwale, A., & Fremling, C. 2022, TNSCR, [2022-1410](#), [1](#)  
 Srivastav, S., Fulton, M., Moore, T., et al. 2022b, TNSAN, [61](#), [1](#)  
 Srivastav, S., Fulton, M., Moore, T., & Yaron, O. 2022a, TNSCR, [2022-667](#), [1](#)  
 Srivastav, S., Gillanders, J., Fulton, M., et al. 2021b, TNSAN, [11](#), [1](#)  
 Srivastav, S., Smartt, S. J., McBrien, O., et al. 2021a, TNSCR, [2021-277](#), [1](#)  
 Stone, N. C., & Metzger, B. D. 2016, *MNRAS*, [455](#), [859](#)  
 Strauss, M. A., Weinberg, D. H., Lupton, R. H., et al. 2002, *AJ*, [124](#), [1810](#)  
 Tachibana, Y., & Miller, A. A. 2018, *PASP*, [130](#), [128001](#)  
 Tadhunter, C., Spence, R., Rose, M., Mullaney, J., & Crowther, P. 2017, *NatAs*, [1](#), [0061](#)  
 Team, S. 2021, TNSCR, [2021-1198](#), [1](#)  
 Terwel, J. 2021a, TNSCR, [2021-2128](#), [1](#)  
 Terwel, J. 2021b, TNSCR, [2021-2152](#), [1](#)  
 Terwel, J., Deckers, M., Dimitriadis, G., et al. 2021c, TNSAN, [227](#), [1](#)  
 Terwel, J., Deckers, M., Harvey, L., Dimitriadis, G., & Irani, I. 2021a, TNSCR, [2021-2952](#), [1](#)  
 Terwel, J., Harvey, L., Prentice, S., et al. 2021b, TNSAN, [50](#), [1](#)  
 Tinyanont, S., Taggart, K., & Foley, R. J. 2021, TNSCR, [2021-1750](#), [1](#)  
 Trakhtenbrot, B., Arcavi, I., Ricci, C., et al. 2019, *NatAs*, [3](#), [242](#)  
 Tucker, M. A. 2021a, TNSCR, [2021-913](#), [1](#)  
 Tucker, M. A. 2021b, TNSCR, [2021-1718](#), [1](#)  
 Valenti, S., Sand, D., Pastorello, A., et al. 2013, *MNRAS: Lett.*, [438](#), [L101](#)  
 van Velzen, S., Holoien, T. W. S., Onori, F., Hung, T., & Arcavi, I. 2020, *SSRv*, [216](#), [124](#)  
 Villar, V. A., Berger, E., Miller, G., et al. 2019, *ApJ*, [884](#), [83](#)  
 Villar, V. A., Hosseinzadeh, G., Berger, E., et al. 2020, *ApJ*, [905](#), [94](#)  
 Wang, J., & Merritt, D. 2004, *ApJ*, [600](#), [149](#)  
 Williams, S. C., Kravtsov, T., Gutierrez, C., et al. 2021b, TNSAN, [98](#), [1](#)  
 Williams, S. C., Kravtsov, T., Gutierrez, C., Nagao, T., & Yaron, O. 2021a, TNSCR, [2021-900](#), [1](#)  
 Yao, Y. 2021, TNSCR, [2021-2295](#), [1](#)  
 Yao, Y. 2022, TNSCR, [2022-2102](#), [1](#)  
 Yao, Y., Brightman, M., Gezari, S., et al. 2021, TNSAN, [183](#), [1](#)  
 York, D. G., Adelman, J., Anderson, J. E. J., et al. 2000, *AJ*, [120](#), [1579](#)